NATIONAL ADVISORY COMMITTEE FOR AERONAUTICS

REPORT 955

APPLICATION OF RADIAL-EQUILIBRIUM CONDITION TO AXIAL-FLOW COMPRESSOR AND TURBINE DESIGN

By CHUNG-HUA WU and LINCOLN WOLFENSTEIN

1950

E R R A T A

NACA REPORT 955

APPLICATION OF RADIAL-EQUILIBRIUM CONDITION TO AXIAL-FLOW COMPRESSOR AND TURBINE DESIGN

By Chung-Hua Wu and Lincoln Wolfenstein

Page 3, paragraph 1 of section "Steady Axially Symmetric Flow" line 4: "steam-turbine theory" should read "hydraulic-machine theory."

Page 4: Equation (21a) should read:

For compression,

$$\eta = \frac{\frac{\gamma - 1}{\gamma}}{\frac{n - 1}{n}} \quad \text{or} \quad n = \frac{1}{1 - \frac{1}{\eta}\frac{\gamma - 1}{\gamma}} \tag{21a}$$

Page 4, right column, line 7: Equation (12) should be equation (13).

Page 11: Equation (53a) should read:

$$\tan \beta = -Kr \tag{53a}$$

NACA-Langley - 12-15-50 - 1600

REPORT 955

APPLICATION OF RADIAL-EQUILIBRIUM CONDITION TO AXIAL-FLOW COMPRESSOR AND TURBINE DESIGN

By CHUNG-HUA WU and LINCOLN WOLFENSTEIN

Lewis Flight Propulsion Laboratory
Cleveland, Ohio

873599—50——1

National Advisory Committee for Aeronautics

Headquarters, 1724 F Street NW, Washington 25, D. C.

Created by act of Congress approved March 3, 1915, for the supervision and direction of the scientific study of the problems of flight (U. S. Code, title 50, sec. 15). Its membership was increased from 12 to 15 by act approved March 2, 1929, and to 17 by act approved May 25, 1948. The members are appointed by the President, and serve as such without compensation.

HUGH L. DRYDEN, PH. D., *Director*

JOHN W. CROWLEY, JR., B. S., *Associate Director for Research*

JOHN F. VICTORY, LL. D., *Executive Secretary*

E. H. CHAMBERLIN, *Executive Officer*

HENRY J. REID, D. Eng., Director, Langley Aeronautical Laboratory, Langley Field, Va.

SMITH J. DEFRANCE, B. S., Director Ames Aeronautical Laboratory, Moffett Field, Calif.

EDWARD R. SHARP, Sc. D., Director, Lewis Flight Propulsion Laboratory, Cleveland Airport, Cleveland, Ohio

---

TECHNICAL COMMITTEES

AERODYNAMICS
POWER PLANTS FOR AIRCRAFT
AIRCRAFT CONSTRUCTION
OPERATING PROBLEMS
INDUSTRY CONSULTING

Coordination of Research Needs of Military and Civil Aviation
Preparation of Research Programs
Allocation of Problems
Prevention of Duplication
Consideration of Inventions

LANGLEY AERONAUTICAL LABORATORY, Langley Field, Va.

LEWIS FLIGHT PROPULSION LABORATORY, Cleveland Airport, Cleveland, Ohio

AMES AERONAUTICAL LABORATORY Moffett Field, Calif.

Conduct, under unified control, for all agencies, of scientific research on the fundamental problems of flight

---

OFFICE OF AERONAUTICAL INTELLIGENCE, Washington, D. C.

Collection, classification, compilation, and dissemination of scientific and technical information on aeronautics

REPORT 955

APPLICATION OF RADIAL-EQUILIBRIUM CONDITION TO AXIAL-FLOW COMPRESSOR AND TURBINE DESIGN

By Chung-Hua Wu and Lincoln Wolfenstein

SUMMARY

Basic general equations governing the three-dimensional compressible flow of gas through a compressor or turbine are given in terms of total enthalpy, entropy, and velocity components of the gas. Two methods of solution are obtained for the simplified, steady axially symmetric flow; one involves the use of a number of successive planes normal to the axis of the machine and short distances apart, and the other involves only three stations for a stage in which an appropriate radial-flow path is used. Methods of calculation for the limiting cases of zero and infinite blade aspect ratios and an approximate method of calculation for finite blade aspect ratio are also given. In these methods, the blade loading and the shape of the annular passage wall may be arbitrarily specified.

The analysis shows that the radial motion of gas consists of a gradual, generally monotone component due to the taper in the passage wall, and an oscillatory component due to the radial variation of the specific mass flow at different stations along the axis of the machine specified in the design. The streamline is curved by this radial flow and a corresponding radial pressure gradient is required to maintain this curvature. The magnitude of this gradient is increased with high Mach number of gas flow and high aspect ratio of blade row. The conventional method of calculation, in which the effect of radial motion on the radial distribution of gas state is neglected, is found to be applicable only for the limiting case of zero aspect ratio.

An analysis of the equations governing the flow shows that a designer is free to prescribe a reasonable radial variation of one of the velocity components or other thermodynamic properties of the gas at any station within the blade region. The various ways of using this degree of freedom and the different types of design obtained are discussed. Numerical computations are then made for two types of compressor and one type of turbine. The results indicate that, even in the case of nontapered passage walls, appreciable radial motion occurs and the corresponding effects are of significant magnitude and should be considered in design.

INTRODUCTION

The design of a compressor or a turbine (either of which is referred to hereinafter as "a turbomachine") may be divided into two phases. The first phase concerns the type of design to be used, or the determination of the most desirable possible variations of velocity and thermodynamic properties of the gas in planes normal to the axis of the machine between successive blade rows. The second phase concerns the design of blades that will give the desired variations of velocity and other properties of gas in these planes. In the first phase, the condition of radial equilibirum (that is, the radial component of the equation of motion) must be used. The flow of gas in a turbomachine is curvilinear; it is curved not only by the whirling motion of gas, but also by the radial motion of the gas (reference 1). The equation of motion then specifies the radial pressure gradient required to provide the centripetal force to maintain the curved flow.

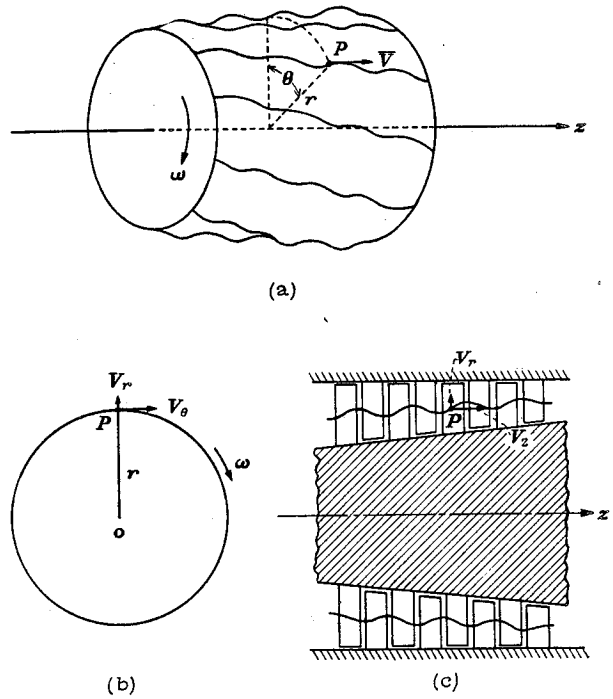

(a) Stream surface over four stages of multistage turbomachine.
(b) Intersection of stream surface with plane normal to axis.
(c) Intersection of stream surface with axial plane.

FIGURE 1.—Stream surface over four similar stages of multistage turbomachine and intersection of stream surface with planes normal to and containing axis of machine.

In figure 1(a), a curved stream surface over four similar stages of a multistage turbomachine is shown and figures 1(b) and 1(c) show the intersections of this stream surface with planes normal to and containing the axis of the machine, respectively. The radial pressure gradient due to the

whirling motion of gas is always positive; whereas that due to the radial motion of gas may be either positive or negative, depending on whether the curvature caused by the motion is inward or outward from the axis of the machine at the point of consideration. Even when the radial motion involved is small, if the gas velocity is high and the blade aspect ratio is large, the radial pressure gradient due to the radial motion is of significant magnitude compared with that due to the whirling motion of gas and should be included in the design calculation.

In the calculation of the state of gas in the normal planes far upstream and downstream of a single row of blades, where the radial motion is small, the pressure gradient is essentially due to the whirling motion alone. Experimental measurement checked well with the calculation when only the whirling motion was considered (references 1 to 3). For the general case of the gas in the normal planes between closely spaced successive blade rows, however, no satisfactory theory exists to calculate the magnitude of the radial displacement of the streamlines and its effect on the radial distribution of the state of the gas. A preliminary theoretical investigation of this problem conducted at the NACA Lewis laboratory was completed in April 1948 and is presented herein.

In the analysis, the general equations governing the three-dimensional flow of gas in turbomachines are expressed in terms of total enthalpy, entropy, and velocity components of the gas. They are developed primarily for the case of steady axially symmetric flow corresponding to the limiting case of an infinite number of blades. Two numerical methods of solution are presented; one uses a number of successive stations through the turbomachine, the other uses only three stations for a stage in which an appropriate radial-flow path is employed.

Methods of solution for the limiting cases of very small and very large blade aspect ratio are then discussed. An approximate solution of the radial displacement across a blade row having a finite aspect ratio is given for the general case in which the whirling velocity of gas is prescribed in design.

The basic equations obtained are also used to investigate the maximum compatible number of radial variations of the velocity components and other thermodynamic properties of gas that a designer is free to specify. It is found that the designer can specify only one such variation at each station along the axis of the machine within the blade region. Various ways of specifying this variation and the different types of design obtained are discussed.

The methods developed are applied to two types of compressor and one type of turbine, in order to investigate the magnitude of the radial motion and its effect on design calculations.

FORMULATION OF EQUATIONS

GENERAL BASIC EQUATIONS

The three-dimensional compressible flow of gas through a turbomachine is governed by the following set of general basic equations (references 4 to 6):

From the principle of conservation of matter, the equation of continuity is

$$\frac{\partial \rho}{\partial t}+\nabla\cdot(\rho\overline{V})=0 \tag{1}$$

(Symbols used in this report are defined in appendix A.) The principle of conservation of momentum is expressed by the Navier-Stokes equation as

$$\rho\frac{D\overline{V}}{Dt}=\rho\overline{F}-\nabla p+\mu\nabla^2\overline{V}+\frac{\mu}{3}\nabla(\nabla\cdot\overline{V})+2[(\nabla\mu)\cdot\nabla]\overline{V}+(\nabla\mu)\times(\nabla\times\overline{V})-\frac{2}{3}(\nabla\cdot\overline{V})(\nabla\mu) \tag{2}$$

where $\overline{F}$ is the external force exerted on unit mass of gas. The principle of conservation of energy may be written as

$$\frac{Du}{Dt}+p\frac{D(\rho^{-1})}{Dt}=Q+\frac{\Phi}{\rho} \tag{3}$$

where u is related to T by

$$\frac{Du}{Dt}=c_v\frac{DT}{Dt} \tag{4}$$

when conduction only is considered, Q is given by

$$Q=\rho^{-1}\nabla\cdot(k\nabla T) \tag{5}$$

and Φ is the dissipation function given by

$$\Phi=\mu\left\{2\nabla\cdot[(\overline{V}\cdot\nabla)\overline{V}]+(\nabla\times\overline{V})^2-2(\overline{V}\cdot\nabla)(\nabla\cdot\overline{V})-\frac{2}{3}(\nabla\cdot\overline{V})^2\right\} \tag{6}$$

For the range of gas temperature and pressure usually encountered in turbomachines, p, ρ, and T are accurately related by the following equation of state:

$$p=R\rho T \tag{7}$$

Theoretically, the preceding seven equations, together with the given body force, known variations of c_v, μ, and k with temperature, and suitable boundary and initial conditions, completely determine the flow of gas through the turbomachine. It is found convenient in the present investigation, however, to base the calculation on total enthalpy and entropy, which are defined by

$$H=h+\frac{1}{2}V^2 \tag{8}$$

where

$$h=u+p\rho^{-1} \tag{9}$$

and

$$T\,ds=du+p\,d(\rho^{-1}) \tag{10}$$

By use of equations (8) to (10), the following forms of continuity, motion, and energy equations are obtained (appendix B):

$$\nabla\cdot\overline{V}+\frac{1}{\gamma-1}\frac{D}{Dt}\log_e T-\frac{D}{Dt}\left(\frac{s}{R}\right)=0 \tag{1a}$$

$$\nabla H=F+T\nabla s+\overline{V}\times(\nabla\times\overline{V})-\frac{\partial\overline{V}}{\partial t}+\frac{\mu}{\rho}\left[\nabla^2\overline{V}+\frac{1}{3}\nabla(\nabla\cdot\overline{V})\right]+$$

$$\frac{1}{\rho}\left\{2[(\nabla\mu)\cdot\nabla]\overline{V}+(\nabla\mu)\times(\nabla\times\overline{V})-\frac{2}{3}(\nabla\cdot\overline{V})(\nabla\mu)\right\} \tag{2a}$$

$$\frac{DH}{Dt}=Q+\frac{\Phi}{\rho}+\frac{1}{\rho}\frac{\partial p}{\partial t}+\overline{V}\cdot\left(\overline{F}+\frac{\mu}{\rho}\left[\nabla^2\overline{V}+\frac{1}{3}\nabla(\nabla\cdot\overline{V})\right]+\right.$$

$$\left.\frac{1}{\rho}\left\{2[(\nabla\mu)\cdot\nabla]\overline{V}+(\nabla\mu)\times(\nabla\times\overline{V})-\frac{2}{3}(\nabla\cdot\overline{V})(\nabla\mu)\right\}\right) \tag{3a}$$

$$\frac{Ds}{Dt}=\frac{Q}{T}+R\frac{\Phi}{p} \tag{3b}$$

Equation (1a) gives the continuity relation in terms of velocity, temperature, and entropy of gas. Equation (2a) relates the gradient of total enthalpy with body force, viscous forces, velocity, and other properties of the gas. This vector equation gives three scalar equations in three dimensions. Equation (3a) gives the rate of change of total enthalpy of gas along a streamline in terms of rate of heat additions, rate of work done by body and viscous forces, and so forth. Equation (3b) gives the rate of change of entropy along a streamline in terms of rate of heat conduction and of dissipation of energy due to viscosity.

STEADY AXIALLY SYMMETRIC FLOW

The solution of the preceding general equations with a given set of suitable boundary and initial conditions is extremely difficult. Useful results may be obtained by considering, as first done by Lorenz in steam-turbine theory (references 7 and 8), the limiting case of an infinite number of infinitesimally thin blades. In this simplification, the force exerted on the gas by a blade element at any radius is considered to be uniformly distributed over the stream sheet between two neighboring blades at that radius, and is considered the body force $\overline{F}$ in the previous equations. For incompressible and frictionless flow, the value thus obtained gives an average value in the circumferential direction, provided the departure from the average value is small (reference 1). Because the number of blades is usually large, this simplification is considered to be reasonable and is also used in the present investigation. For steady inlet and exit conditions, all partial derivatives with respect to angular coordinate θ and time t are then equal to zero and the state of gas is a function of r and z only.

The ideal case of a nonviscous gas will be considered first. In this case, there exist two more relations defining the problem. One is the fact that blade force is normal to the surface of the blade and, consequently, to the relative velocity of gas or the relative stream surface; that is,

$$\overline{F}\cdot(\overline{V}-\overline{U})=0 \tag{11}$$

or, referring to absolute cylindrical coordinates r, θ, z and the relative angular coordinate χ,

$$F_r dr+rF_\theta d\chi+F_z\,dz=0 \tag{11a}$$

The other is the condition of integrability of the blade surface,

$$\overline{F}\cdot(\nabla\times\overline{F})=0 \tag{12}$$

which in the case of axial symmetry reduces to (references 8 and 9)

$$\frac{\partial}{\partial r}\left(\frac{F_z}{rF_\theta}\right)=\frac{\partial}{\partial z}\left(\frac{F_r}{rF_\theta}\right) \tag{12a}$$

From the general equations (1a), (2a), (3a), and (3b), and equations (11) and (12a), the following equations are obtained for steady axially symmetric flow of nonviscous gas: (See appendix B.)

$$\frac{1}{r}\frac{\partial(rV_r)}{\partial r}+\frac{\partial V_z}{\partial z}+\frac{1}{\gamma-1}\left(V_r\frac{\partial}{\partial r}\log_e T+V_z\frac{\partial}{\partial z}\log_e T\right)-$$

$$\left[V_r\frac{\partial}{\partial r}\left(\frac{s}{R}\right)+V_z\frac{\partial}{\partial z}\left(\frac{s}{R}\right)\right]=0 \tag{13}$$

$$\frac{\partial H}{\partial r}=F_r+T\frac{\partial s}{\partial r}+\frac{V_\theta}{r}\frac{\partial(rV_\theta)}{\partial r}+V_z\left(\frac{\partial V_z}{\partial r}-\frac{\partial V_r}{\partial z}\right) \tag{14}$$

$$0=F_\theta-\frac{1}{r}\left[V_r\frac{\partial(rV_\theta)}{\partial r}+V_z\frac{\partial(rV_\theta)}{\partial z}\right] \tag{15}$$

$$\frac{\partial H}{\partial z}=F_z+T\frac{\partial s}{\partial z}+\frac{V_\theta}{r}\frac{\partial(rV_\theta)}{\partial z}-V_r\left(\frac{\partial V_z}{\partial r}-\frac{\partial V_r}{\partial z}\right) \tag{16}$$

$$\frac{DH}{Dt}=Q+\omega\frac{D(rV_\theta)}{Dt} \tag{18}$$

$$\frac{\partial}{\partial r}\left(\frac{F_z}{rF_\theta}\right)=\frac{\partial}{\partial z}\left(\frac{F_r}{rF_\theta}\right) \tag{12a}$$

In the preceding equations, equation (13) is the continuity equation; equations (14), (15), and (16) are the three equations of motion in the radial, circumferential, and axial directions, respectively. Equation (17) is considered to represent the energy equation and equation (18) to represent equation (11). In these equations, Q is now the heat transfer from the blade to the gas, uniformly distributed in the circumferential direction, as is the blade force $\overline{F}$. These seven equations are considered seven independent equations that relate the eight unknown variables, which consist of three blade-force components, three velocity components, and H and s of the gas. The first three quantities determine

the shape of the blade and the last five quantities completely determine the state of the gas (all other thermodynamic properties of gas, such as p, ρ, and T, can be computed from them by using equations (7) to (10)).

For compressors and turbines without blade cooling, the heat transfer between blade and gas is negligible; the entropy of gas is then constant along any streamline according to the energy equation (17). If the inlet air has a uniform value of entropy, the radial and axial derivatives of entropy in the preceding equations equal zero.

In the case of real gas, the axially symmetric simplified forms of the viscous terms in equations (1a), (2a), (3a), and (3b) can be obtained in a similar manner. These terms in the equations of motion may be neglected when compared with other terms in the same equation if the boundary layers along the passage walls are relatively thin. Because of the viscous shearing stresses in the gas adjacent to the blade, the force exerted by the blade on the gas is now slightly inclined from the direction normal to the relative velocity of gas and, consequently, equations (11) and (12) are not strictly true (the force components in the equations should be replaced by the direction cosines of the normal to the blade surface). Without using equation (11), however, equation (18) can be obtained from the equation of motion and the energy equation for steady flow with the assumption that the heat generated from the frictional work remains in each stream sheet (appendix B) and can therefore be considered as representing the energy relation in the set of equations. The entropy increase along the streamline is then computed from a consideration of the actual compression or expansion process

$$p=K\rho^n \tag{19}$$

by the formula (appendix B)

$$\frac{ds}{dt}=-R\frac{n-\gamma}{(n-1)(\gamma-1)}\left(V_r\frac{\partial}{\partial r}\log_e T+V_z\frac{\partial}{\partial z}\log_e T\right) \tag{20}$$

In equation (20), n is constant along a streamline. In a given machine, n may be directly obtained from pressure and temperature data. In a new design, n must be obtained from the assumed polytropic efficiency used in design calculations for uncooled blades:

For compression,

$$\eta=\frac{\dfrac{\gamma-1}{\gamma}}{\dfrac{n-1}{n}} \quad \text{or} \quad n=\frac{1}{1-\dfrac{1}{\eta}\dfrac{\gamma-1}{\gamma}} \tag{21a}$$

For expansion,

$$\eta=\frac{\dfrac{n-1}{n}}{\dfrac{\gamma-1}{\gamma}} \quad \text{or} \quad n=\frac{1}{1-\eta\dfrac{\gamma-1}{\gamma}} \tag{21b}$$

Because the change in s is usually small compared with the changes in H and V, the preceding method of determining s may be adequate to account for the viscous effect in calculating the pressure and density change along the streamline for the present problem. This correction is more important in the case of multistage compressors. For a viscous fluid, equation (20) therefore replaces equation (17) in the previous set of equations; and equations (14), (15), (16), (18), and (12a) are considered approximately true. With equation (12), there are still seven independent equations defining the flow and the shape of the blade.

METHODS OF SOLUTION

The preceding section presents seven independent equations relating the eight dependent variables V_r, V_θ, V_z, H, s, F_r, F_θ, and F_z, which define the flow of gas and the blade shape in the blade region. In the direct problem with a given machine, the shape of the blade section provides one more relation between F_θ and F_z, giving eight relations to determine the variation of the eight quantities throughout the blade region. In the inverse problem, an appropriate desirable variation of any one quantity is prescribed within the blade region; the preceding seven equations then determine the variation of the remaining seven quantities throughout the blade region. No general solution of these equations seems possible, however, in either problem. Two numerical methods of solution are therefore suggested. In the first method, the preceding equations are applied to successive planes normal to the axis of the machine and short distances apart; this method is applicable to both direct and inverse problems. In the second method, a particular case is considered, in which a simple appropriate radial-flow path is prescribed in the design. This method may also be used as a simple approximate solution in a direct problem in which the radial-flow path is approximately known.

METHOD OF FINITE DIFFERENCE FOR SUCCESSIVE AXIAL STATIONS

When two successive stations j and k a short distance apart within the blade are considered (fig. 2) and rV_θ is denoted by ζ, equations (14) to (16) may be written for each station as

$$\frac{\partial H}{\partial r}=F_r+T\frac{\partial s}{\partial r}+\frac{\zeta}{r^2}\frac{\partial \zeta}{\partial r}+V_z\left(\frac{\partial V_z}{\partial r}-\frac{\partial V_r}{\partial z}\right) \tag{14a}$$

$$0=F_\theta-\frac{1}{r}\left(V_r\frac{\partial \zeta}{\partial r}+V_z\frac{\partial \zeta}{\partial z}\right) \tag{15a}$$

$$\frac{\partial H}{\partial z}=F_z+T\frac{\partial s}{\partial z}+\frac{\zeta}{r^2}\frac{\partial \zeta}{\partial z}-V_r\left(\frac{\partial V_z}{\partial r}-\frac{\partial V_r}{\partial z}\right) \tag{16a}$$

The change in total enthalpy and entropy between the two stations is obtained from equations (18) and (20) (appendix B):

$$H_k(r_k)-H_j(r_j)=\omega[\zeta_k(r_k)-\zeta_j(r_j)]+\int_{t_j}^{t_k}Q\,dt \tag{18a}$$

$$s_k(r_k)-s_j(r_j)=R\frac{n-\gamma}{(n-1)(\gamma-1)}\log_e\frac{H_k-\dfrac{V_k^2}{2}}{H_j-\dfrac{V_j^2}{2}} \tag{20a}$$

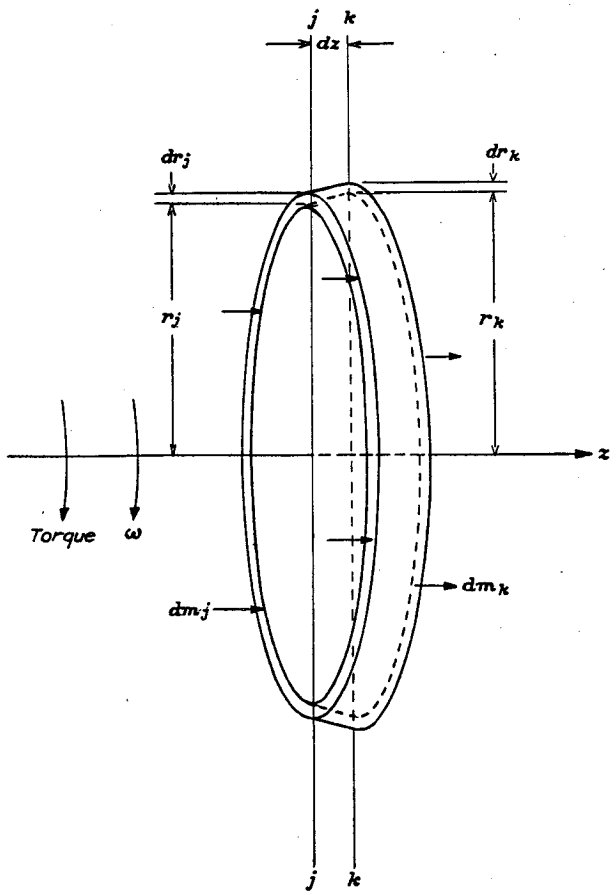

FIGURE 2.—Stations j and k short distance apart.

where (r) indicates that the gas properties at a particular station are a function of the radial position of the gas particle in that station. (It should be noted that because of radial motion, the radial position of a gas particle at any station k is different from its radial position at the previous station j.)

Instead of integrating equation (13), the continuity relation between the two stations is readily obtained by equating the mass flow at the two stations:

$$G_k r_k\, dr_k = G_j r_j\, dr_j \tag{22}$$

By expressing G in terms of H, V, and s, equation (22) becomes (appendix B)

$$V_{z,k}\left(H_k-\frac{V_k^2}{2}\right)^{\frac{1}{\gamma-1}} e^{-\frac{s_k}{R}} r_k\, dr_k = V_{z,j}\left(H_j-\frac{V_j^2}{2}\right)^{\frac{1}{\gamma-1}} e^{-\frac{s_j}{R}} r_j\, dr_j \tag{22a}$$

Equations (12a), (14a), (15a), (16a), (18a), (20a), and (22a) are now seven independent equations relating the gas properties and the blade forces at the two stations in the blade region. In these equations, the heat transfer is negligible in an ordinary turbomachine and can be estimated in the case of cooled turbine blades; the temperature T is a known function of H, V, and s; n is given; and r_k is obtained from r_j and $V_{r,j}$. Hence, there are only eight unknowns in H, s, V_r, V_θ, V_z, F_r, F_θ, and F_z at the second station k. In the direct problem, the blade shape gives one more relation between F_θ and F_z; whereas in the inverse problem, one suitable relation among the eight unknowns is specified by the designer. In either case, the unknowns at station k can be obtained from the known values at station j, the passage-wall shape, and the preceding relations.

In the free space between two blade rows, or in the space upstream of the first blade row and downstream of the last blade row, the force terms drop out of the equations, which results in equation (22a) and the following equations (neglecting friction and heat transfer between gas and passage wall):

$$\frac{\partial H}{\partial r}=T\frac{\partial s}{\partial r}+\frac{\zeta}{r^2}\frac{\partial \zeta}{\partial r}+V_z\left(\frac{\partial V_z}{\partial r}-\frac{\partial V_r}{\partial z}\right) \tag{14b}$$

$$0=V_r\frac{\partial \zeta}{\partial r}+V_z\frac{\partial \zeta}{\partial z}=\frac{D\zeta}{Dt} \tag{15b}$$

$$\frac{\partial H}{\partial z}=T\frac{\partial s}{\partial z}+\frac{\zeta}{r^2}\frac{\partial \zeta}{\partial z}-V_r\left(\frac{\partial V_z}{\partial r}-\frac{\partial V_r}{\partial z}\right) \tag{16b}$$

$$\frac{Ds}{Dt}=0 \tag{20b}$$

Equation (22a) and these four independent equations, together with the given passage-wall shape, completely determine the variations of the five independent quantities V_r, V_θ, V_z, H, and s outside the blade region. The solution of the problem over the entire region inside and outside the blade region, using this step-by-step method, varies with the type of design and the condition given or prescribed. In any case, the computation would be quite laborious.

In order to obtain an over-all picture of the radial flow in a turbomachine and its effect on design consideration in a simpler way, the following method considering the problem of a particular case is given:

METHOD OF PRESCRIBED RADIAL-FLOW PATH

In a turbomachine, the radial motion of the gas is caused by three factors:

(1) Tapering of the annular passage either at the inner or outer wall gives the flow a radial displacement across the stage, which is, of course, greatest in the immediate neighborhood of the tapered surface.

(2) Even with a nontapered passage, a radial displacement across the stage may be necessary because of a variation in the distribution of specific mass flow over the blade height across the stage.

(3) Even if no radial displacement occurs across the stage (that is, the same particle occupies the same radial position at the first station of each successive stage), there will, in general, be radial displacement of flow within the stage. This radial flow will then be oscillatory in nature, a radial displacement in the rotor being followed by an equal and

opposite radial displacement in the stator. This radial flow arises because of the difference between the radial variation of the specific mass flow within the stage and that at the entrance and exit stations of the stage. (This radial displacement can only be avoided by specifying zero or the same radial variation of specific mass flow at all stations of the stage in the design.)

In general, the radial flow of gas therefore consists of a gradual, generally monotone, radial motion due to factors (1) and (2), with an oscillatory motion of period equal to the stage length due to factor (3) superimposed on it. The radial flow caused by these three factors will be similar to that shown in figure 1. The effect of the radial motion on the calculations arises chiefly through the term $\partial V_r/\partial z$ in the radial-equilibrium equation (14a). This term is expected to be significant mainly because of the oscillatory motion, which may require significant changes in V_r within a single row of blades. The case of oscillatory motion within a stage with no over-all radial displacement across the stage will therefore be considered first. That is, the gas-passage wall is nontapered and the radial distribution of gas properties at the entrance and exit stations of the stage is the same.

Because there is no blade force acting on the gas, the gas flowing through the gap between two blades is under a nearly constant pressure gradient and consequently tends to move with the same curvature it acquires while leaving the first blade. For nontapered passages, the maximum or minimum point of the radial-flow path is likely to be somewhere near the middle of the gap. (The intersecting curve of a stream surface with an axial plane is herein referred to as "the radial-flow path." Because of axial symmetry, the radial-flow path is the same in any axial plane.) The stations between blade rows are most conveniently chosen at these points. The stations in front of the rotor, between the rotor and the stator, and behind the stator are denoted by subscripts 1, 2, and 3, respectively. (See fig. 3(a).) If r_o and L represent the mean radial distance of the flow path and the axial length of the blade row, respectively, then the radial distance of the gas particle at position z is given by

$$r-r_o=-\frac{r_2-r_1}{2}f\left(\frac{z}{L}\right) \tag{23}$$

and at stations 1, 2, and 3, $z/L=0, 1, 2$

$$\left.\begin{aligned} &f(0)=f(2)=1, f(1)=-1\\ &f'(0)=f'(1)=f'(2)=0 \end{aligned}\right\} \tag{24}$$

where f is a function giving the form of the radial-flow path and the prime indicates differentiation with respect to z/L. It follows that

$$V_r=V_z\frac{dr}{dz}=-\frac{r_2-r_1}{2L}V_z f'\left(\frac{z}{L}\right) \tag{25}$$

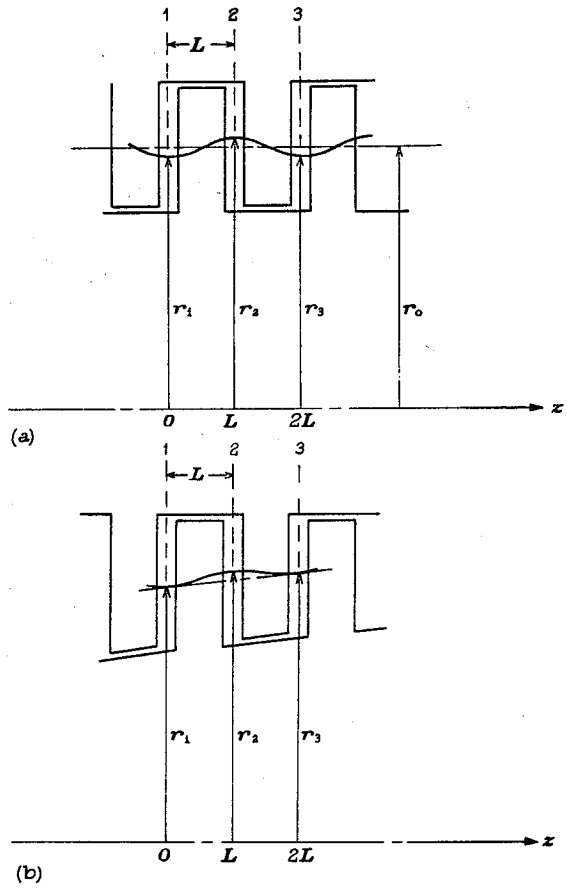

(a) Nontapered passage.
(b) Tapered passage.
FIGURE 3.—Stations between blade rows.

At station 1, $z=0$,

$$V_{r,1}=0$$

and

$$\left(\frac{\partial V_r}{\partial z}\right)_1=-\frac{r_2-r_1}{2L^2}V_{z,1}f''(0) \tag{26}$$

inasmuch as $\partial V_z/\partial z$ is practically zero in passing through the gap. Similarly, at station 2, $z=L$,

$$V_{r,2}=0$$

and

$$\left(\frac{\partial V_r}{\partial z}\right)_2=-\frac{r_2-r_1}{2L^2}V_{z,2}f''(1) \tag{27}$$

Because $f''(z/L)$ determines $\partial V_r/\partial z$ or the effect of radial motion on the radial-equilibrium condition, it is desirable that it vary continuously; this condition together with those of equations (24) suggests

$$f\left(\frac{z}{L}\right)=\cos\pi\left(\frac{z}{L}\right)$$

Then

$$f''(0)=-\pi^2,\ f''(1)=\pi^2$$

and equations (23) and (25) to (27) become, respectively,

$$r-r_o=-\frac{r_2-r_1}{2}\cos\pi\left(\frac{z}{L}\right) \tag{23a}$$

$$V_r=\pi\frac{r_2-r_1}{2L}V_z\sin\pi\left(\frac{z}{L}\right) \tag{25a}$$

$$\left(\frac{\partial V_r}{\partial z}\right)_1=\pi^2\frac{r_2-r_1}{2L^2}V_{z,1} \tag{26a}$$

$$\left(\frac{\partial V_r}{\partial z}\right)_2=-\pi^2\frac{r_2-r_1}{2L^2}V_{z,2} \tag{27a}$$

For the sinusoidal form of $f(z/L)$, the maximum absolute value of $f''(z/L)$ occurs at $z=0$, L, and $2L$, and is equal to π^2. Even if $f''(z/L)$ is assumed constant between $z=0$ and $z=L/2$, thus minimizing the maximum absolute value of f'' in the interval, the absolute value of f'' equals 8. This assumption, however, necessitates a discontinuity in f'' at $z=L/2$. The values of π^2 for the absolute values of $f''(0)$ and $f''(1)$ can therefore be considered as small as is likely. The smooth variation of $f''(z/L)$ and the minimization of the absolute value of $f''(z/L)$ at the stations make it desirable to employ equation (23a) in the design. This simple radial-flow path will also give a good approximate answer to most designs in which the distribution of blade loading and radial blade force is not too ununiform in the axial direction. In such cases, this simple sinusoidal curve is believed to represent the major harmonic of the actual radial-flow path and the principal effect of the radial motion may be obtained through the use of this simple curve.

The radial-equilibrium equation (14b) may be written in terms of (r_2-r_1) by use of equations (26a) and (27a)

$$\frac{dH_i}{dr_i}=T_i\frac{ds_i}{dr_i}+\frac{\zeta_i}{r_i^2}\frac{d\zeta_i}{dr_i}+V_{z,i}\frac{dV_{z,i}}{dr_i}+(-1)^i\pi^2\frac{r_2-r_1}{2L^2}V_{z,i}^2 \tag{14c}$$

where

$$i=1,2,3$$

When r_i is replaced by the dimensionless variable $r_i'=\left(\frac{r_i}{r_t-r_h}\right)$, equation (14c) becomes

$$\frac{dH_i}{dr_i'}=T_i\frac{ds_i}{dr_i'}+\frac{1}{r_i'^2}\frac{\zeta_i}{r_t-r_h}\frac{d}{dr_i'}\left(\frac{\zeta_i}{r_t-r_h}\right)+V_{z,i}\frac{dV_{z,i}}{dr_i'}+(-1)^i\frac{\pi^2}{2}(r_2'-r_1')A^2V_{z,i}^2 \tag{14d}$$

This form of the radial-equilibrium equation is seen to contain a term directly proportional to the radial displacement, to the square of the axial velocity, and to the square of the blade-row aspect ratio. If the blade-row aspect ratio is large or the axial velocity is high, the effect of radial motion may be large even though only a small amount of radial displacement occurs across the blade row.

This method is readily extended to the case where an overall radial displacement occurs across the stage due to tapering of the passage or due to variation in the design from stage to stage. In figure 3(b), the radial position of a gas particle originally at r_1 in station 1 is at r_3 in station 3. For the oscillatory motion required within the stage, r_2 is not generally equal to $\frac{1}{2}(r_1+r_3)$. For the same reason stated in the previous case, it is desirable to have the radial-flow path consisting of a sinusoidal curve superimposed on the line passing through (z_1, r_1) and (z_3, r_3); that is,

$$r=r_1+\frac{r_3-r_1}{2}\frac{z}{L}+\frac{1}{2}\left(r_2-\frac{r_1+r_3}{2}\right)\left(1-\cos\frac{\pi z}{L}\right) \tag{23b}$$

Then

$$V_r=\left[\frac{r_3-r_1}{2L}+\frac{\pi}{2L}\left(r_2-\frac{r_1+r_3}{2}\right)\sin\frac{\pi z}{L}\right]V_z \tag{25b}$$

and

$$-\left(\frac{\partial V_r}{\partial z}\right)_i=(-1)^i\frac{\pi^2}{2L^2}\left(r_2-\frac{r_1+r_3}{2}\right)V_{z,i} \tag{26b}$$

inasmuch as $\partial V_z/\partial z$ is practically zero in passing through the gap. With this value of $\partial V_r/\partial z$, the radial-equilibrium equation (14b) becomes

$$\frac{dH_i}{dr_i}=T_i\frac{ds_i}{dr_i}+\frac{\zeta_i}{r_i^2}\frac{d\zeta_i}{dr_i}+V_{z,i}\frac{dV_{z,i}}{dr_i}+(-1)^i\frac{\pi^2}{2L^2}\left(r_2-\frac{r_1+r_3}{2}\right)V_{z,i}^2 \tag{14e}$$

This equation is similar to equation (14c). (If $r_3=r_1$, it reduces to equation (14c).) A similar equation in dimensionless r_i' can also be obtained for this case by dividing r_i by $(r_t-r_h)_i$.

With this method of prescribed radial-flow path, if it is only required to find the velocity distribution in stations between successive blade rows (to provide data for the design or setting of blades), the distribution can be obtained by considering only these planes without making any computation in the blade regions. For example, suppose that all quantities are known at the inlet station of the stage (station 1), then for station 2 behind the rotor blade row the following relations exist: When the untapered passage walls are considered, equations (14c), (18a), (20b), and (22a) give

$$\frac{dH_2}{dr_2}=T_2\frac{ds_2}{dr_2}+\frac{\zeta_2}{r_2^2}\frac{d\zeta_2}{dr_2}+V_{z,2}\frac{dV_{z,2}}{dr_2}+\pi^2\frac{r_2-r_1}{2L^2}V_{z,2}^2 \tag{14f}$$

$$H_2(r_2)=H_1(r_1)+\omega[\zeta_2(r_2)-\zeta_1(r_1)]+\int_{t_1}^{t_2}Q\,dt \tag{18b}$$

$$s_2(r_2)=s_1(r_1)+R\frac{n-\gamma}{(n-1)(\gamma-1)}\log_e\frac{H_2-\frac{1}{2}V_2^2}{H_1-\frac{1}{2}V_1^2} \tag{20c}$$

and

$$V_{z,2}\left(H_2-\frac{1}{2}V_2^2\right)^{\frac{1}{\gamma-1}}e^{-\frac{s_2}{R}}r_2\,dr_2=V_{z,1}\left(H_1-\frac{1}{2}V_1^2\right)^{\frac{1}{\gamma-1}}e^{-\frac{s_1}{R}}r_1\,dr_1 \tag{22b}$$

If the radial variation of one quantity is known (such as $\partial\zeta_2/\partial r_2=0$, $\partial V_{z,2}/\partial r_2=0$, or $\partial\beta_2/\partial r_2=0$) among the five unknowns at station 2 (consisting of ζ_2, $V_{z,2}$, H_2, s_2, and $r_2(r_1)$), all the other quantities can be determined. The procedure will vary with different types of design. In most cases, the computation may be started with an appropriate value of r_2 as a function of r_1 obtained by an approximate solution. With the variation of one of the four quantities H_2, s_2, ζ_2, and $V_{z,2}$ given, the remaining three quantities are computed from equations (14f), (18b), and (20c). These values are then inserted in equation (22b) to determine if the continuity relation is satisfied. If it is not, the values must be adjusted until the continuity relation is satisfied. An alternative procedure is to insert these values in equation (C5), which is derived from equation (22b), to obtain new values of r_2 as a function of r_1, and the entire process is repeated until the desired accuracy is reached. In a tapered passage, both stations 2 and 3 must be computed at the same time. An application of this method to a nonvortex-type compressor stage will be given in the section **NUMERICAL EXAMPLES FOR TYPICAL DESIGNS.**

LIMITING CASES AND APPROXIMATE SOLUTIONS

Simplified-radial-equilibrium approximation.—In this commonly used approximation, the gas is assumed to flow on cylindrical surfaces for nontapered passage walls; that is,

$$\left.\begin{aligned} V_r&=0\\ r_1&=r_2=r_3 \end{aligned}\right\} \tag{28}$$

At these stations, the radial-equilibrium equation (14b) reduces to

$$\frac{dH_i}{dr_i}=T_i\frac{ds_i}{dr_i}+\frac{\zeta_i}{r_i^2}\frac{d\zeta_i}{dr_i}+V_{z,i}\frac{dV_{z,i}}{dr_i} \tag{14g}$$

where $i=1$, 2, or 3.

For tapered passage walls, a certain simple relation among r_1, r_2, and r_3 is assumed, but the term containing $\partial V_r/\partial z$ in the radial-equilibrium equation is still neglected (that is, equation (14g) is used instead of equation (14b)).

With this simplifying assumption, the gas state at station 2 or 3 can be computed much more easily from the gas state at station 1 and the one condition specified at stations 2 and 3. The continuity equation (22b) for individual stream sheets, however, is now discarded because of the assumed relation among r_1, r_2, and r_3 and is replaced by the following continuity relation for the entire annular area:

$$\int_{r_{2,h}}^{r_{2,t}}G_2r_2\,dr_2=\int_{r_{1,h}}^{r_{1,t}}G_1r_1\,dr_1 \tag{22c}$$

Thus, equations (14g), (18b), and (20c) are used in this calculation, with equation (22c) used as a check on total mass flow.

When ds_i/dr_i is negligible, the following equations for the radial variations of pressure and density can be obtained from equations (14g), (B4), and (B8):

$$\frac{p_{t,i}^{\frac{1}{\gamma}}}{\rho_{t,i}}\,p_i^{-\frac{1}{\gamma}}\frac{dp_i}{dr_i}=\frac{V_{\theta,i}^2}{r_i}-V_{r,i}\frac{dV_{r,i}}{dr_i} \tag{29}$$

$$\gamma\frac{p_{t,i}}{\rho_{t,i}^{\gamma}}\,\rho_i^{\gamma-2}\frac{d\rho_i}{dr_i}=\frac{V_{\theta,i}^2}{r_i}-V_{r,i}\frac{dV_{r,i}}{dr_i} \tag{30}$$

In these two equations, the last term is very small compared with the next-to-last term and may therefore be neglected. Under the present assumption, this term becomes zero for a nontapered passage and the resulting equation may be more directly obtained, as is usually done, by taking the approximation involved in the use of

$$\frac{1}{\rho_i}\frac{dp_i}{dr_i}=\frac{V_{\theta,i}^2}{r_i}$$

for the equation of motion in the radial direction in place of

$$\frac{1}{\rho_i}\frac{dp_i}{dr_i}=\frac{V_{\theta,i}^2}{r_i}-V_{z,i}\left(\frac{\partial V_r}{\partial z}\right)_i-V_{r,i}\frac{dV_{r,i}}{dr_i}$$

Equations derived from this basis of calculation in dimensionless forms are given in appendix D for several types of design.

Limiting case of zero aspect ratio.—Two limiting cases will now be discussed for which the evaluation of the term $\left(\frac{\partial V_r}{\partial z}\right)_i$ can be avoided. If the blade row has an axial length sufficiently great relative to the radial length (that is, if the blade-row aspect ratio is sufficiently small), the term $\left(\frac{\partial V_r}{\partial z}\right)_i$ will be negligible in spite of any radial displacement across the blade row. This extreme situation is designated the zero-aspect-ratio case and differs from the simplified-radial-equilibrium approximation in that the radial displacement across the blade row is properly determined and its effect on the state of gas is included in the calculation. The continuity equation (22b) for individual stream sheets is therefore to be satisfied in addition to equation (22c), but equation (14g) is still used in place of (14c). In the case of gas-passage walls having no taper or slight taper, the difference between the two cases is small; a successive-approximation procedure starting with the result of the simplified-radial-equilibrium calculation can therefore be used. This procedure may be outlined as follows:

1. With the given values at station 1 and one prescribed condition at station 2, use the simplified-radial-equilibrium equations to find ζ_2, $V_{z,2}$, H_2, and s at station 2 as functions of r_1; then compute $G_2(r_1)$.
2. By using the value of $G_2(r_1)$ obtained from step 1, find $r_2(r_1)$ from equation (C5).
3. Substitute this value of $r_2(r_1)$ into equations (14g), (18b), and (20c) to obtain a second solution for ζ_2, $V_{z,2}$, H_2, and s_2 as functions of r_1.
4. Repeat steps 2 and 3 if necessary, using the value of $G_2(r_1)$ obtained from step 3.

In the case where there is considerable taper at the passage walls, it is better to assume $r_2(r_1)$ according to the taper to start the calculation rather than to use steps 1 and 2.

Limiting case of infinite aspect ratio.—The other limiting case corresponds to a blade row with axial length negligible as compared with radial length, and is designated the infinite-aspect-ratio case. The negligible axial length does not provide space for any appreciable radial displacement, hence r_2 may be taken as equal to r_1, or

$$G_2=G_1 \tag{31}$$

and for a tapered passage, either the preceding equation or a relation similar to the one that follows may be used:

$$G_2=G_1\frac{r_{1,t}^2-r_{1,h}^2}{r_{2,t}^2-r_{1,h}^2} \tag{32}$$

Either of these two equations now takes the plaee of the continuity equation (22b).

Because the change in axial length for a very small change in V_r is also very small, $(\partial V_r/\partial z)_t$ does not vanish. Although its absolute value does not affect the radial motion because of the negligible blade-row axial length, the relative value of $\partial V_r/\partial z$ ahead of and behind a blade row is needed to determine completely the distribution of gas properties at these stations. If the loading of the blade in the axial direction is relatively uniform or the blade is designed to give a sinusoidal radial-flow path, the curvatures of the radial-flow path at the two stations can be considered equal in magnitude and opposite in sense. Then,

$$\left(\frac{\partial V_r}{\partial z}\right)_1=-\left(\frac{\partial V_r}{\partial z}\right)_2 \tag{33}$$

In order to combine this relation with equation (14b) in a simple manner, it may be assumed that

$$V_{z,1}\left(\frac{\partial V_r}{\partial z}\right)_1=-V_{z,2}\left(\frac{\partial V_r}{\partial z}\right)_2 \tag{34}$$

Combining equation (34) with equation (14b) at stations 1 and 2 yields

$$\frac{dH_1}{dr_1}+\frac{dH_2}{dr_2}=T_1\frac{ds_1}{dr_1}+T_2\frac{ds_2}{dr_2}+\frac{\zeta_1}{r_1}\frac{d\zeta_1}{dr_1}+\frac{\zeta_2}{r_2}\frac{d\zeta_2}{dr_2}+$$

$$V_{z,1}\frac{dV_{z,1}}{dr_1}+V_{z,2}\frac{dV_{z,2}}{dr_2} \tag{34a}$$

For a typical stage of a given design, equations (14b), (18b), and (20c), with either equation (31) or (32) and equation (33) or (34) will completely determine the variation of gas properties at the two stations.

In appendix E, formulas are given in dimensionless forms for two common types of design in order to calculate the variations of gas properties for the two preceding limiting cases. The results so obtained will give the limits of the variation of the gas properties along the blade height. If the difference is large, it is worthwhile to make the calculation for the given blade-row aspect ratio.

Approximate solution for finite aspect ratio.—For the general cases where ζ_1 and ζ_2 are prescribed in design as functions of r_1, an approximate solution for the radial displacement across the blade row can be determined in the following manner:

First take as two separate functions

$\Delta_e(r_1)$ the function (r_2-r_1) of r_1 satisfying the radial-equilibrium and total-enthalpy-change equations for a given distribution of the other variables

$\Delta_c(r_1)$ the function (r_2-r_1) of r_1 satisfying continuity equation (22) for a given distribution of other variables

It is assumed in this method that the radial gradients in V_z and ζ depend primarily on the magnitude of the radial displacement (r_2-r_1) and not on its exact distribution. Accordingly,

$$\Delta_e(r_1)=y_e\ g(r_1) \tag{35}$$

where y_e is the maximum value of Δ_e and $g(r_1)$ is a plausible form for the distribution of Δ_e satisfying the boundary conditions:

$$\text{for}\quad \left.\begin{aligned} &g(r_{1,h})=g(r_{1,t})=0\\ &g'(r_{1,m})=0, g(r_{1,m})=1\end{aligned}\right\} \tag{36}$$

If Δ_c is calculated for several values of Δ_e, it is possible to plot y_c, the maximum value of Δ_c, against y_e. A fairly good approximate solution might be expected to correspond to the point $y_c=y_e$. This process can be further refined by varying $g(r_1)$ from the function originally assumed in the direction of the calculated function Δ_c/y_c.

By the use of this procedure, the following approximate value for the magnitude of radial displacement across a blade row is obtained (appendix F):

$$r_2-r_1=\frac{(r_2-r_1)_s}{1+A^2} \tag{37}$$

This value can be used as a starting value for exact calculations or may be used as the final value for approximate calculations.

APPLICATION TO DESIGN

DEGREE OF FREEDOM IN DESIGN

In the preceding analysis it was shown that within the blade region there are only seven independent equations relating the eight dependent variables that determine the state of gas and the blade shape; whereas in the space outside the blade, there are five independent equations that determine the five dependent variables determining the state of gas. In the inverse or design problem, the designer therefore has one and only one degree of freedom for prescribing a reasonable radial variation of one single quantity in all blade regions, of a different quantity in different blade regions, or a single relation between several quantities. In addition, he is free to specify the taper in the passage wall, the position where the radial element of the blade is set, and a suitable condition of gas at stations far ahead of and behind the machine as boundary conditions, such as a uniform state of gas entering the machine.

In current design practice, design computation is made only in the planes between successive blade rows in which a certain desirable variation of one gas property can be specified. The blades are then either selected from cascade data or theoretically designed to achieve the calculated gas states in these stations. For this reason, the following discussion of different ways of specifying these variations will be centered in these planes: For simplicity, only the adiabatic case is considered. Under this condition, if equation (18a) is applied to the three successive stations of a stage and is differentiated with respect to r_1,

$$\frac{dH_1}{dr_1}+\omega\left(\frac{d\zeta_2}{dr_2}\frac{dr_2}{dr_1}-\frac{d\zeta_1}{dr_1}\right)=\frac{dH_2}{dr_2}\frac{dr_2}{dr_1}=\frac{dH_3}{dr_3}\frac{dr_3}{dr_1} \tag{38}$$

A few ways of taking up the degrees of freedom at these stations between successive blade rows are listed in the following paragraphs:

(1) Constant work per unit mass of gas flow over the blade height. This condition is usually specified in the design of a turbomachine. It relates ζ behind the rotor to its value ahead of the rotor by

$$\zeta_2(r_2)=\zeta_1(r_1)+r_{1,t}\delta_t U_{1,t} \tag{39}$$

or

$$\frac{d\zeta_2}{dr_2}\frac{dr_2}{dr_1}=\frac{d\zeta_1}{dr_1} \tag{39a}$$

where $r_{1,t}\delta_t U_{1,t}$ is equal to $(\zeta_2-\zeta_1)$ at the blade tip and is also equal to $(\zeta_2-\zeta_1)$ at other radii.

Constant work over the blade height gives constant total-enthalpy change over the blade height. If the velocity at the exit of a stage is equal to that at the entrance, this condition also gives constant static-enthalpy change over the blade height.

Under the condition of constant work, equation (38) reduces to

$$\frac{dH_1}{dr_1}=\frac{dH_2}{dr_2}\frac{dr_2}{dr_1}=\frac{dH_3}{dr_3}\frac{dr_3}{dr_1} \tag{38a}$$

(2) Constant total enthalpy over the blade height:

$$\frac{\partial H}{\partial r}=0 \tag{40}$$

This condition usually applies to the first stage of a compressor and will hold for all succeeding stages if constant work per unit mass over the blade height is employed. If a nonzero value of dH_1/dr_1 is desired, an initial preparatory stage must be specially designed to obtain this value. In the last stage, however, it is usually desirable that $\partial H/\partial r$ be nearly zero.

(3) Free-vortex-type distribution of tangential velocity:

$$\frac{\partial\zeta}{\partial r}=0 \tag{41}$$

or

$$\zeta_i=K_i \tag{41a}$$

This condition is commonly used in turbines and compressors. Ignoring radial motion, in addition to this condition, constant total enthalpy and constant axial velocity over the blade height can be obtained. Considering radial motion, only one of these two additional conditions can be obtained in conjunction with equation (41). (See section **NUMERICAL EXAMPLES FOR TYPICAL DESIGNS.**)

(4) Symmetrical velocity diagram. If $V_{z,1}=V_{z,2}$ and $r_1=r_2=r$, the symmetrical velocity diagram gives

$$V_{\theta,1}+V_{\theta,2}=\omega r \tag{42}$$

or

$$\zeta_1+\zeta_2=\omega r^2 \tag{42a}$$

Differentiating with respect to r yields

$$\frac{d\zeta_1}{dr}+\frac{d\zeta_2}{dr}=2\omega r \tag{42b}$$

If $r_1\neq r_2$ or $V_{z,1}\neq V_{z,2}$, the symmetrical velocity diagrams may be defined by

$$\zeta_1(r_1)+\zeta_2(r_2)=\omega r_1^2 \tag{43}$$

Then,

$$\frac{d\zeta_1}{dr_1}+\frac{d\zeta_2}{dr_1}=2\omega r_1 \tag{43a}$$

With the use of the symmetrical velocity diagram, the aerodynamic limitations of gas flow through the rotor and the stator are reached at about the same time. Reference 10 shows that the blade-profile loss is a minimum with the symmetrical velocity diagram if the lift-drag ratio is constant. For incompressible flow, the change in static pressure or enthalpy is also the same in passing through the rotor or the stator, and the stage is therefore often referred to as the "50-percent reaction stage."

(5) Wheel-type distribution of tangential velocity:

$$V_{\theta,i}=K_i r_i \tag{44}$$

or

$$\frac{d\zeta_i}{dr_i}=2K_i r_i \tag{44a}$$

(6) Constant tangential velocity:

$$V_{\theta,i}=K_i \tag{45}$$

$$\frac{d\zeta_i}{dr_i}=K_i \tag{45a}$$

(7) Constant axial velocity over blade height:

$$\frac{\partial V_z}{\partial r}=0 \tag{46}$$

At a very low speed of gas flow with no change in density, the specific mass flow will also be constant over the blade height; there will therefore be no radial flow across the blade row and equation (14b) reduces to (with the entropy variation neglected)

$$\frac{\partial H}{\partial r}-\frac{\zeta}{r^2}\frac{\partial\zeta}{\partial r}=0 \tag{47}$$

And when

$$\frac{\partial H}{\partial r}=0$$

$$\frac{\partial \zeta}{\partial r}=0$$

The equivalence of equations (46) and (47) breaks down, however, for current aircraft applications, where the speed of gas flow is high.

If equation (47) is substituted into the radial-equilibrium equation (14b) with entropy variation neglected, the following relation is obtained:

$$\frac{\partial V_z}{\partial r}-\frac{\partial V_r}{\partial z}=0 \tag{47a}$$

The left side of equation (47a) is the tangential component of fluid rotation $\nabla\times\overline{V}$; thus equation (47) is a condition for potential flow in the free space between blade rows.

If it is desired to take into account in design the effect of the boundary layers at the inner and outer walls of the gas passage, instead of equation (46) an appropriate axial-velocity variation close to the actual one may be prescribed in design:

$$\frac{dV_{z,i}}{dr_i}=\varphi_i(r_i) \tag{46a}$$

(8) Constant specific mass flow over blade height. In order to avoid radial movement across the blade row in compressible flow, it has been suggested (for example, reference 11) that constant axial velocity be replaced by constant specific mass flow:

$$\frac{dG_1}{dr}=\frac{dG_2}{dr}=\frac{dG_3}{dr}=0 \tag{48}$$

Radial displacement can also be prevented by the use of two conditions instead of three:

$$\frac{dG_1}{dr}=\frac{dG_2}{dr}=\frac{dG_3}{dr} \tag{49}$$

For designs using either of these two conditions, the simplified-radial-equilibrium calculation is more correct. Designs employing no radial flow have the advantage that the calculation does not involve any radial displacement across the blade row and that the two-dimensional-cascade data can be directly applied. The final equations derived from these conditions (equations (48) or (49)), however, are difficult to solve and the conditions are incompatible with tapered passage in a multistage turbomachine.

(9) Relative Mach number. For high performance, a certain variation of relative Mach number consistent with the radial variation of solidity and thickness of blade may be specified in design. Then for the rotor,

$$\frac{V_{z,1}^2+(V_{\theta,1}-\omega r_1)^2}{(\gamma-1)\left[H_1-\frac{1}{2}\left(V_{z,1}^2+V_{\theta,1}^2\right)\right]}=M_1^2=\varphi_1(r_1) \tag{50}$$

For the stator,

$$\frac{V_{z,2}^2+V_{\theta,2}^2}{(\gamma-1)\left[H_2-\frac{1}{2}\left(V_{z,2}^2+V_{\theta,2}^2\right)\right]}=M_2^2=\varphi_2(r_2) \tag{51}$$

(10) Untwisted rotor blades. For simplicity in fabrication, especially for a cooled turbine, untwisted rotor blades may be used. Inasmuch as the flow angle is only slightly different from the blade angle, the following relation may be used in design:

$$\left.\begin{aligned}\frac{d\beta_1}{dr_1}&=0\\ \frac{d\beta_2}{dr_2}&=0\end{aligned}\right\} \tag{52}$$

(11) Blades with all elements radial. For high-speed rotor blades, in order to reduce centrifugal stress it may be desirable to have all blade elements radial. Then,

$$F_r=0 \tag{53}$$

By using this relation, equation (12a) reduces to

$$\frac{F_z}{F_\theta}=Kr$$

or

$$\tan\beta=Kr \tag{53a}$$

where K is a function of z.

In multistage machines, similar variation in either tangential velocity, axial velocity, or specific mass flow may be specified at the similar stations of each stage:

$$\frac{d\zeta_1}{dr_1}=\frac{d\zeta_3}{dr_3}\frac{dr_3}{dr_1} \tag{54}$$

$$\frac{dV_{z,1}}{dr_1}=\frac{dV_{z,3}}{dr_3}\frac{dr_3}{dr_1} \tag{55}$$

or

$$\frac{dG_1}{dr_1}=\frac{dG_3}{dr_3}\frac{dr_3}{dr_1} \tag{56}$$

Stages of multistage machines designed for similar variations of gas properties from stage to stage are termed "typical stages."

Types of design.—A large number of different types of design may be obtained by different combinations of those conditions specified in equations (39) to (56). These designs may be conveniently divided into two groups. In the first group, the condition of constant work at all radii is specified in the design. That is, equation (39) is employed, which gives:

$$\left.\begin{aligned}&\frac{d\zeta_1}{dr_1}=\frac{d\zeta_2}{dr_1}\\ \text{and}\quad&\frac{dH_1}{dr_1}=\frac{dH_2}{dr_1}=\frac{dH_3}{dr_1}\end{aligned}\right\}\qquad(57).$$

In cases where the symmetrical velocity diagram is also specified, by using equation (43a), equation (57) reduces to

$$\left.\begin{aligned}&\frac{d\zeta_1}{dr_1}=\frac{d\zeta_2}{dr_1}=\omega r_1\\ \text{and}\quad&\frac{dH_1}{dr_1}=\frac{dH_2}{dr_1}=\frac{dH_3}{dr_1}\end{aligned}\right\}\qquad(58)$$

In the second group, the condition of constant work is not specified.

The following tables present a few types of design in each of the two groups for multistage turbomachines consisting of a number of similar stages. The manner in which the degree of freedom is used up at each station of a typical stage and the known characteristics of each type are given. The typical stage is considered to consist of a rotor followed by a stator.

These conditions specified for the typical stage, as given in the table, completely determine the flow over all the stages. The flow in the inlet guide vane, if required, is to be determined by the given condition at the inlet to the machine and the condition specified at station 1. Similarly, the flow in the last stator is to be determined by the condition specified behind the last rotor and the given condition at the exit of the machine.

It may be desirable for certain applications to use different types of design in a multistage unit. Those designs can be obtained by using only the relations of different types at stations 1 and 2 in the table.

GROUP I

Type	Station	Conditions specified at 3 stations of any stage	Characteristics of flow		Additional remarks
1. Free vortex	1 2 3	$\frac{d\zeta_1}{dr_1}=0$ Constant work $\frac{d\zeta_1}{dr_1}=\frac{d\zeta_3}{dr_1}$	$\frac{d\zeta_1}{dr_1}=\frac{d\zeta_2}{dr_2}=\frac{d\zeta_3}{dr_3}=0$ $\frac{dH_1}{dr_1}=\frac{dH_2}{dr_1}=\frac{dH_3}{dr_1}$	$V_{\theta,i}=K_i/r_i$ Constant axial velocity over blade height for incompressible flow. Small radial gradient in axial velocity for compressible flow.	If $\frac{\partial H}{\partial r}=0$ at inlet to machine, $\frac{\partial H}{\partial r}=0$ at all stations.
2. Symmetrical velocity diagram	1 2 3	Symmetrical velocity diagram Constant work $\frac{d\zeta_1}{dr_1}=\frac{d\zeta_3}{dr_1}$	$\frac{d\zeta_1}{dr_1}=\frac{d\zeta_2}{dr_1}=\frac{d\zeta_3}{dr_1}=\omega r_1$ $\frac{dH_1}{dr_1}=\frac{dH_2}{dr_1}=\frac{dH_3}{dr_1}$	$V_{\theta,1}=\frac{\omega r_1}{2}-\frac{\delta_t U_{1,t}}{2}\frac{r_{1,t}}{r_1}$ $V_{\theta,2}=\left(\frac{\omega r_1}{2}+\frac{\delta_t U_{1,t}}{2}\frac{r_{1,t}}{r_1}\right)\frac{r_1}{r_2}$ Combination of wheel-type and vortex-type tangential velocities. Large negative radial gradient of axial velocity at all stations.	If $\frac{\partial H}{\partial r}=0$ at inlet to machine, $\frac{\partial H}{\partial r}=0$ at all stations.
3. Wheel-type tangential velocity in front of rotor	1 2 3	$\frac{d\zeta_1}{dr_1}=2Kr_1$ Constant work $\frac{d\zeta_1}{dr_1}=\frac{d\zeta_3}{dr_1}$	$\frac{d\zeta_1}{dr_1}=\frac{d\zeta_2}{dr_1}=\frac{d\zeta_3}{dr_1}=2Kr_1$ $\frac{dH_1}{dr_1}=\frac{dH_2}{dr_1}=\frac{dH_3}{dr_1}$	$V_{\theta,1}=Kr_1$ $V_{\theta,2}=\left(Kr_1+\delta_t U_{1,t}\frac{r_{1,t}}{r_1}\right)\frac{r_1}{r_2}$ Large negative radial gradient of axial velocity at all stations.	If $\frac{\partial H}{\partial r}=0$ at inlet to machine, $\frac{\partial H}{\partial r}=0$ at all stations.
4. Same variation in axial velocity	1 2 3	Constant work $\frac{dV_{z,1}}{dr_1}=\frac{dV_{z,2}}{dr_1}$ $\frac{dV_{z,1}}{dr_1}=\frac{dV_{z,3}}{dr_1}$	$\frac{d\zeta_1}{dr_1}=\frac{d\zeta_2}{dr_1}$ $\frac{dH_1}{dr_1}=\frac{dH_2}{dr_1}=\frac{dH_3}{dr_1}$ $\frac{dV_{z,1}}{dr_1}=\frac{dV_{z,2}}{dr_2}=\frac{dV_{z,3}}{dr_3}$	For incompressible flow, this type requires no radial flow across blade rows and is equivalent to first type in group. For compressible flow, small radial gradient exists in ζ.	If $\frac{\partial H}{\partial r}=0$ at inlet to machine, $\frac{\partial H}{\partial r}=0$ at all stations.
5. Same variation in specific mass flow	1 2 3	Constant work $\frac{dG_1}{dr_1}=\frac{dG_2}{dr_1}$ $\frac{dG_1}{dr_1}=\frac{dG_3}{dr_1}$	$\frac{d\zeta_1}{dr_1}=\frac{d\zeta_2}{dr_1}$ $\frac{dH_1}{dr_1}=\frac{dH_2}{dr_1}=\frac{dH_3}{dr_1}$ $\frac{dG_1}{dr_1}=\frac{dG_2}{dr_1}=\frac{dG_3}{dr_1}$	No radial flow across rotor and stator blades for nontapered passage.	If $\frac{\partial H}{\partial r}=0$ at inlet to machine, $\frac{\partial H}{\partial r}=0$ at all stations.

GROUP II

Type	Station	Conditions specified at 3 stations of any stage	Characteristics of flow	
1. Constant specific mass flow	1	$\frac{dG_1}{dr_1}=0$	$\frac{dG_1}{dr_1}=\frac{dG_2}{dr_2}=\frac{dG_3}{dr_3}=0$	No radial flow across all blades in nontapered passage.
	2	$\frac{dG_2}{dr_2}=0$		
	3	$\frac{dG_3}{dr_3}=0$		
2. Constant axial velocity	1	$\frac{dV_{z,1}}{dr_1}=0$	$\frac{dV_{z,1}}{dr_1}=\frac{dV_{z,2}}{dr_2}=\frac{dV_{z,3}}{dr_3}=0$	No radial flow across all blades in nontapered passage for incompressible flow.
	2	$\frac{dV_{z,2}}{dr_2}=0$		
	3	$\frac{dV_{z,3}}{dr_3}=0$		
3. Untwisted rotor blade	1	$\frac{d\beta_1}{dr_1}=0$	$\frac{d\beta_1}{dr_1}=\frac{d\beta_2}{dr_2}=\frac{d\beta_3}{dr_3}=0$	
	2	$\frac{d\beta_2}{dr_2}=0$		
	3	$\frac{d\beta_3}{dr_3}=0$		

NUMERICAL EXAMPLES FOR TYPICAL DESIGNS

The methods of calculation previously outlined are applied to the typical stages of compressors of types 1 and 2 of group I, as given in the table. The inlet total enthalpy is assumed uniform with respect to radius; and with work exchange with rotor uniform along the radius, total enthalpy is constant with respect to radius in all stations. The calculation is rendered dimensionless by expressing all velocities in terms of U_t, total enthalpy in terms of U_t^2, and r in terms of r_t. Because the main purpose of the calculation is to determine the magnitude of the oscillatory radial motion and its effect on the radial distribution of gas properties, a nontapered passage wall is used. Heat transfer is assumed to be zero in the calculation and the entropy is assumed to be constant at each station. The change of entropy across the blades at all radii is assumed equal to that obtained from the polytropic efficiency assumed at the mean radius. This calculation does not take into account the boundary layers at the rotor drum and the outer casing, and consequently is good only for the main portion of gas flowing between them. This restriction can be removed if more data on the variation of n with radius are available.

In the comparison of different blade-row aspect ratios in each design, in addition to the same aerodynamic limitations, the same axial velocity at the mean radius is used. The comparison between different cases will be slightly different if another basis of comparison is used.

Symmetrical-velocity-diagram and constant-total-enthalpy compressor.—Because the difference between zero- and infinite-aspect-ratio cases is found to be large in this design, two calculations are made for a blade-row aspect ratio of 2; one calculation is based on a prescribed sinusoidal radial-flow path, the other is based on the approximate solution of equation (37). The equations based on prescribed sinusoidal radial-flow path are given in appendix G. The following design constants are used for all cases:

Hub-tip ratio	0.6
Limiting Mach number relative to rotor blade	0.8
Limiting value of $\frac{V_{\theta,2}-V_{\theta,1}}{V_{z,1}}$	0.7
Polytropic efficiency at mean radius	0.9
$V_{z,1,m}/U_t$	0.772

The limiting value of $\frac{V_{\theta,2}-V_{\theta,1}}{V_{z,1}}$ is based on a formula given by Howell (reference 12). The last value results from the use of $V_{z,1,h}/U_t=0.8$ in the simplified-radial-equilibrium calculation, and is used for all cases. The results of the calculation are shown in figure 4.

The distribution of specific mass flow ahead of and behind the rotor for the different cases considered is shown in figure 4(a). It may be seen that in all cases except the infinite-aspect-ratio case, the specific mass flow G/G_t increases toward the hub faster behind the rotor than ahead of the rotor; that is, passing through the rotor, the gas moves toward the axis of the machine. The magnitude of this displacement is obtained from the continuity equation (C5) and is shown in figure 4(b). In the simplified-radial-equilibrium calculation, it is assumed that there is no radial motion, but when the distribution of specific mass flow is substituted in the continuity equation (C5), quite large radial displacement across the blade is obtained. This kind of calculation is therefore inconsistent. In other calculations, the distributions of gas

properties are calculated from assumed radial displacements that are to be checked with the displacements required from the continuity relation with these distributions, and are therefore consistent in themselves. The radial displacement used in the approximate calculation for $A=2$ is obtained by the approximate formula, equation (37), and is about 25 percent lower than the value obtained from using the sinusoidal radial-flow path.

The variation of axial velocities is given in figure 4(c), which shows that the axial velocities increase toward the hub in all cases, but at different rates. The high value of axial velocity at the hub entering the rotor blade allows the use of higher turnings at all radii without exceeding the limiting value of $(V_{\theta,2}-V_{\theta,1})/V_{z,1}$ or σC_L at the hub. It also helps

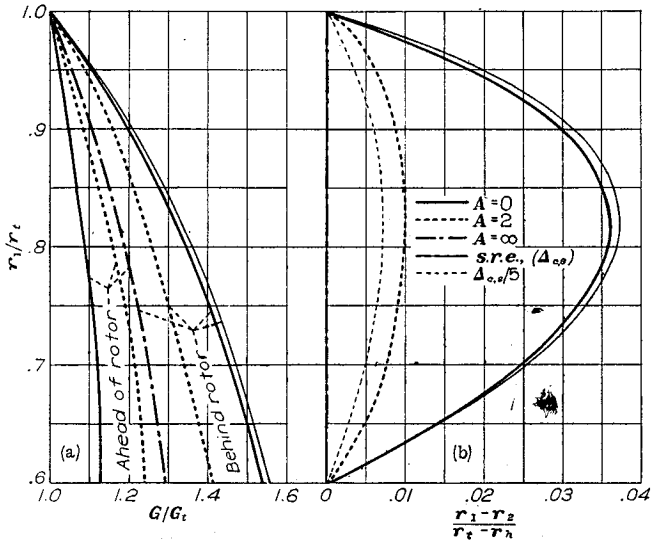

(a) Distribution of specific mass flow. (b) Radial displacement across rotor.

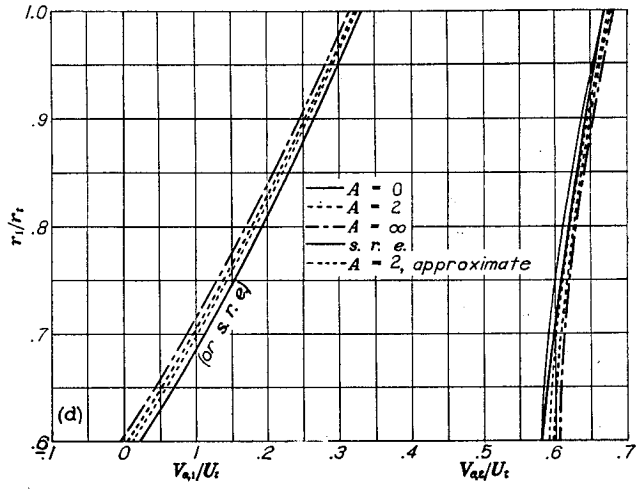

(d) Variation of tangential velocities.

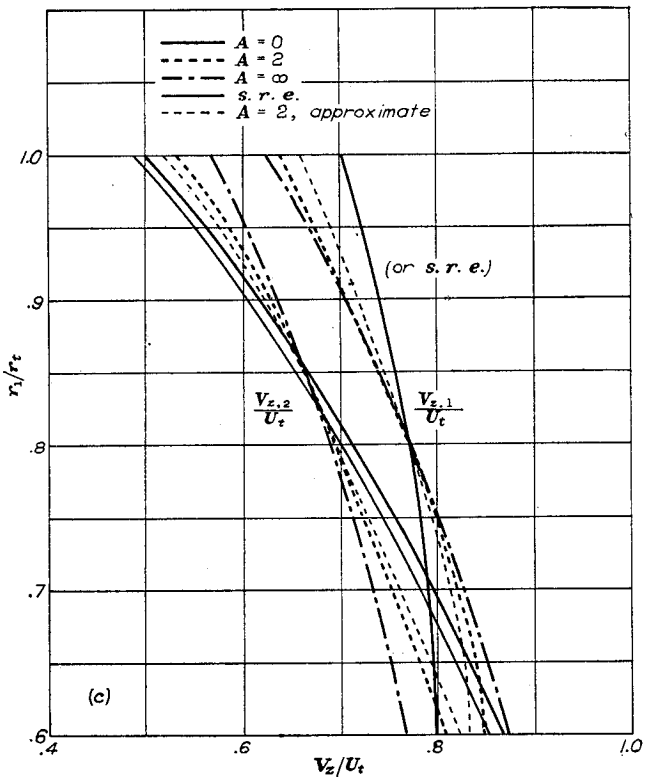

(c) Variation of axial velocities.

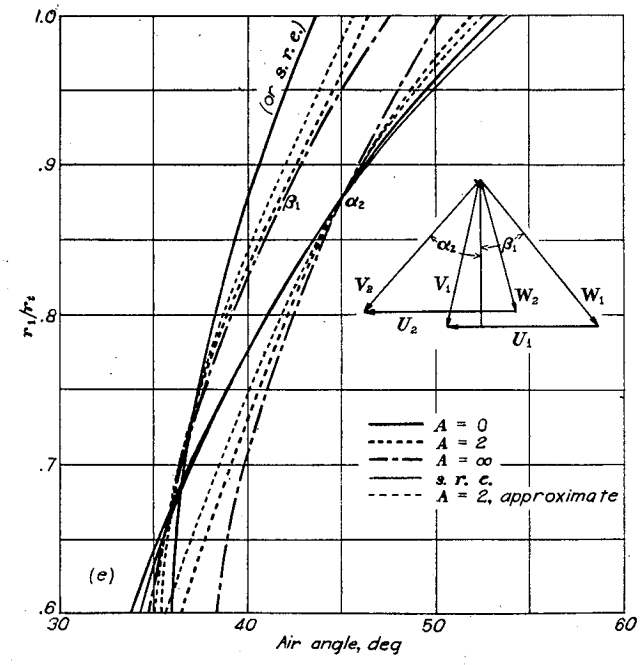

(e) Variation of air angles.

FIGURE 4.—Symmetrical-velocity-diagram and constant-total-enthalpy compressor.

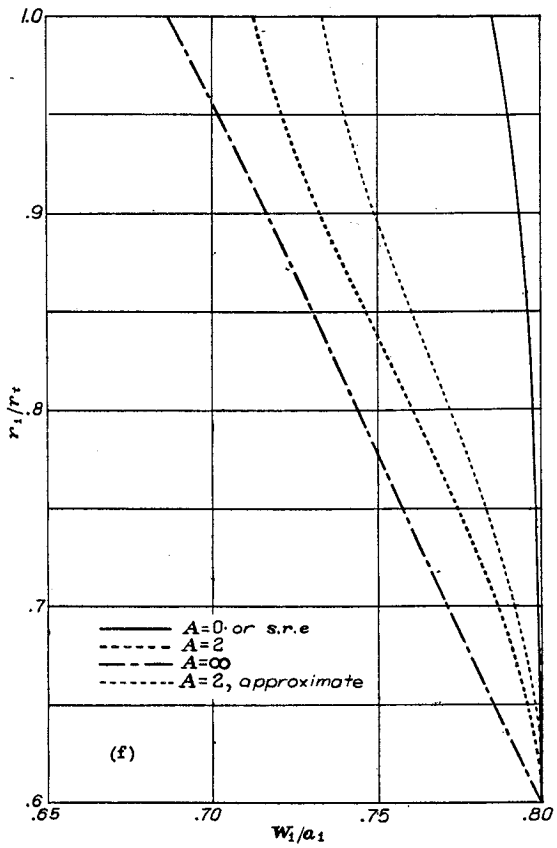

(f) Variation of Mach number relative to rotor blades.

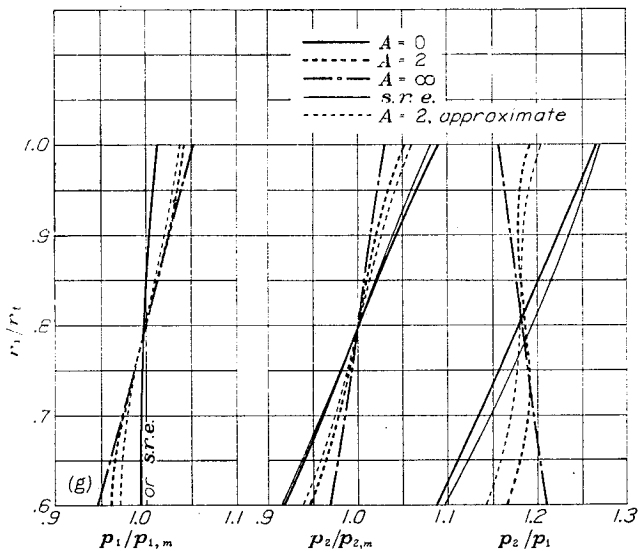

(g) Pressure distributions and pressure rise across rotor.

to give a more uniform Mach number relative to the rotor blade over the blade height. As a result, this type of design gives a higher pressure rise and a higher specific mass flow than a free-vortex type of design using the same design limitations. In order to utilize this advantage fully, the variation of axial velocity should be correctly determined.

The calculation of axial velocity based on simplified radial equilibrium gives a result close to the zero-aspect-ratio case, which is also true in the distribution of other properties in this calculation, because in the case of zero aspect ratio, the curvature caused by radial motion is negligible and the difference in gas properties caused by the radial displacement is very small in the nontapered passage.

The variation of tangential velocities is shown in figure 4(d). These velocities in different cases vary in a similar manner and the difference of magnitude between them is mainly due to the different value of δ_t determined by the different values of $V_{z,1,h}/U_t$ in the various cases.

Figure 4(e) shows the variation of air angles entering the rotor and stator blades. The difference between the simplified-radial-equilibrium calculation and the case of aspect ratio of 2 is significant throughout the whole blade height. The simplified-radial-equilibrium calculation gives a value about 3° lower than the aspect ratio of 2 at the tip of the rotor blade and at the hub of the stator blades.

The variation of Mach number relative to the rotor blades is shown in figure 4(f). The simplified-radial-equilibrium calculation gives a nearly constant value; whereas the more correct calculations show that Mach number actually decreases about 10 percent toward the tip for the case of blade-row aspect ratio equal to 2. (This variation, however, is only about one-third of that of a similar free-vortex compressor.)

The pressure distributions ahead of and behind the rotor and the pressure rise across the rotor at different radii are shown in figure 4(g). The difference in pressure distribu-

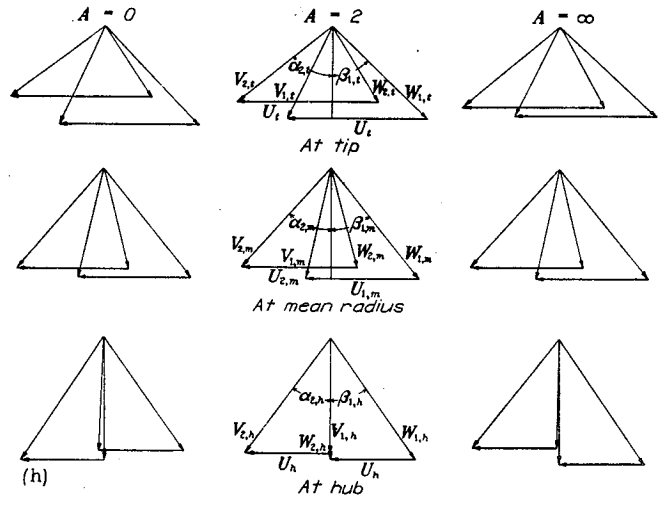

(h) Velocity diagrams at different radii.

FIGURE 4.—Concluded. Symmetrical-velocity-diagram and constant-total-enthalpy compressor.

tions may explain to a certain extent the difference found between measurement and the simplified-radial-equilibrium calculation. The pressure rise across the rotor is fairly uniform in the case of an aspect ratio of 2 and is a desirable feature.

The velocity diagrams at three radii for aspect ratios of 0, 2, and ∞ are shown in figure 4(h). If this stage is used as the first stage of a compressor, the permissible tip rotor speed of this design at standard sea-level conditions is equal to 868 and 826 feet per second for $A=0$ and $A=2$, respectively. The specific mass flow per unit annulus area, corrected to standard sea-level conditions, is equal to 41.5 and 40.0 pounds per square foot per second for $A=0$ and $A=2$, respectively.

Free-vortex and constant-total-enthalpy compressor.—The design constants used are the same as in the previous calculation. In addition, $V_{\theta,1}$ and $V_{\theta,2}$ are considered to be equal to $W_{\theta,2}$ and $W_{\theta,1}$, respectively, at the mean radius. In this type of design, the simplified-radial-equilibrium approximation is equivalent to the zero-aspect-ratio case, because, due

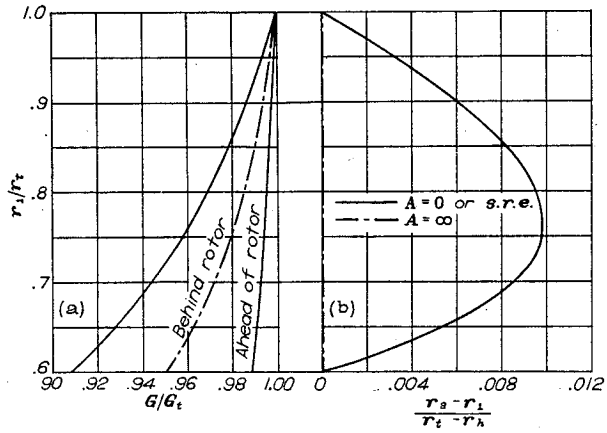

(a) Distribution of specific mass flow. (b) Radial displacement across rotor.

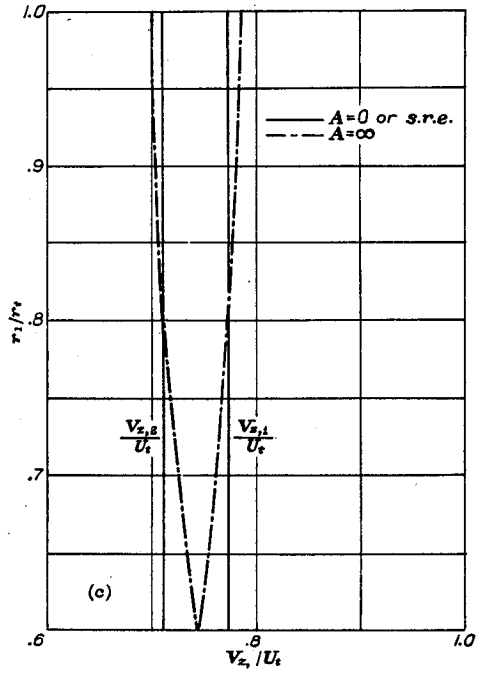

(d) Variation of air angles.

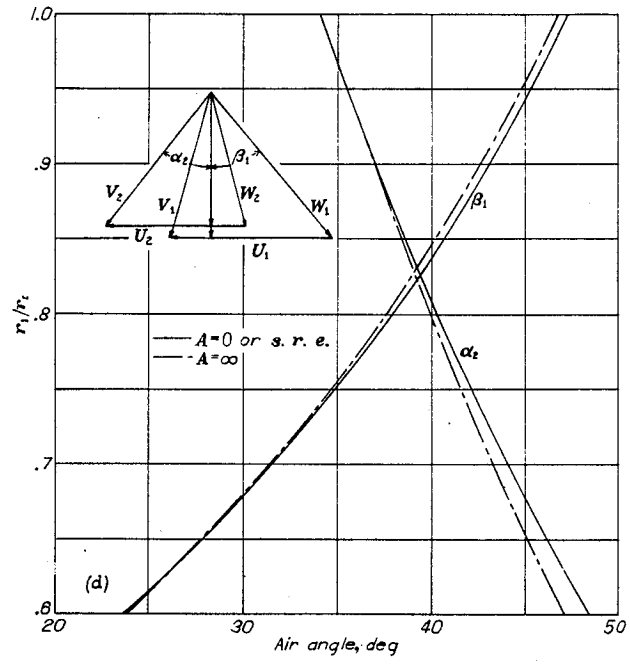

(c) Variation of axial velocities.

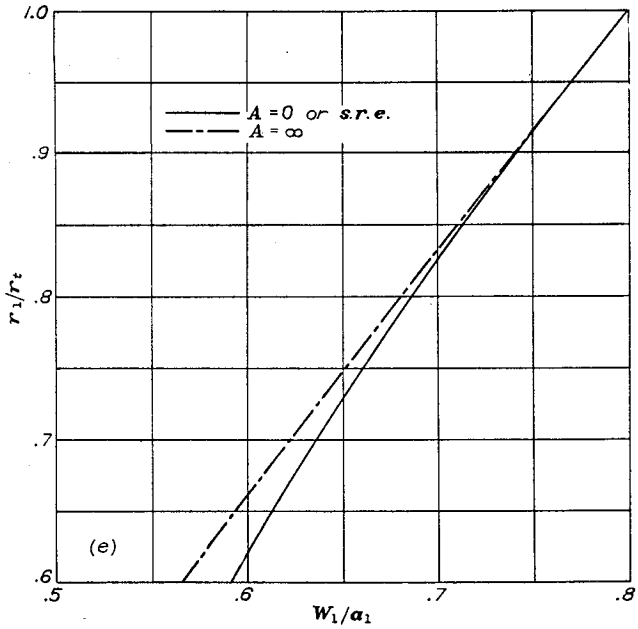

(e) Variation of Mach number relative to rotor blades.

FIGURE 5.—Free-vortex and constant-total-enthalpy compressor.

to the constant value of rV_θ in this design, the radial motion across the blade does not affect the calculation in the zero-aspect-ratio case. That is, the same values of H_1, H_2, ζ_1, ζ_2, $V_{z,1}$, and $V_{z,2}$ occur in both cases and the entire calculation is the same. (See also equation (F6).)

Because the radial motion involved in this type of design is mainly due to the compressibility of gas, the difference between the zero- and infinite-aspect-ratio cases is not large; hence the calculation for a finite-aspect-ratio case is not made.

The distribution of specific mass flow ahead of and behind the rotor is presented in figure 5(a). Even in the zero-aspect-ratio or simplified-radial-equilibrium case with a constant axial-velocity distribution, considerable change occurs in density, which requires an appreciable amount of outward radial motion to obtain the given design conditions behind the rotor. Although the amount of this radial motion is small (fig. 5(b)), its effect on the variation of gas properties is not entirely negligible. Its effect can be seen in the curves of figures 5(c) to 5(g), which are somewhat similar to the symmetrical-velocity-diagram and constant-total-enthalpy design in nature but of smaller magnitudes.

If this stage is used as the first stage of a compressor, the permissible tip rotor speed at standard sea-level conditions is equal to 758 feet per second for $A=0$. This tip speed is about 13 percent lower than that of the corresponding case of the previous design. The specific mass flow corrected to standard sea-level conditions is equal to 38.6 pounds per square foot of annulus area per second for $A=0$, which is 7 percent lower than that of the corresponding case of the previous design.

Free-vortex and constant-total-enthalpy turbine.—The design constants used in the calculation are: $M_t<1$, $U_t/a_{1,t}=0.5$, $V_{\theta,1,h}/a_{1,t}=0.8$, $V_{z,1,m}/a_{1,t}=0.4$, $V_{\theta,2}=0$, and polytropic efficiency at mean radius equal to 0.87. For the simplified-radial-equilibrium approximation or zero aspect ratio, $V_{z,1}/U_t$ is constant and so is $V_{z,2}/U_t$, which is found by the continuity relation to be equal to 0.877. The same velocity at station 2 is used for the infinite aspect ratio, thus making the only difference at station 1. The results of the calculation are shown in figure 6.

The distribution of specific mass flow ahead of and behind the rotor is shown in figure 6(a). Because of the constant axial exit velocity, the specific mass flow is constant behind the rotor. Except for the case of infinite aspect ratio, there is an inward radial motion of gas in passing through the rotor (fig. 6(b)), the magnitude of which is about two and one-half times that in the previous free-vortex compressor (fig. 5(b)).

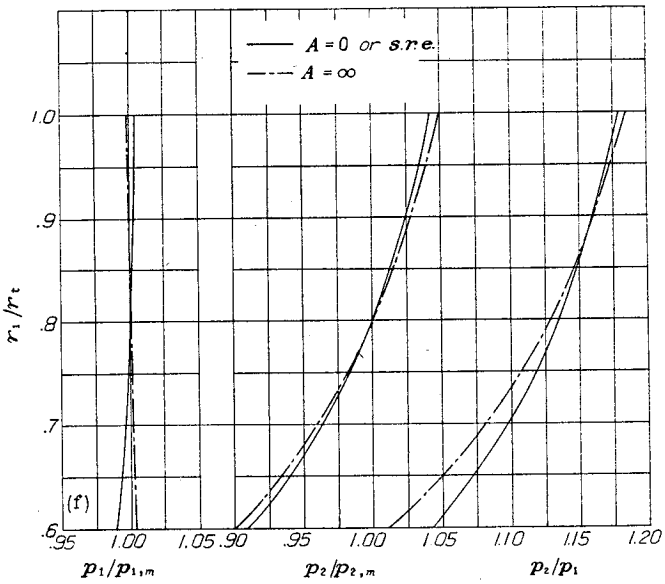

(f) Pressure distributions and pressure rise across rotor.

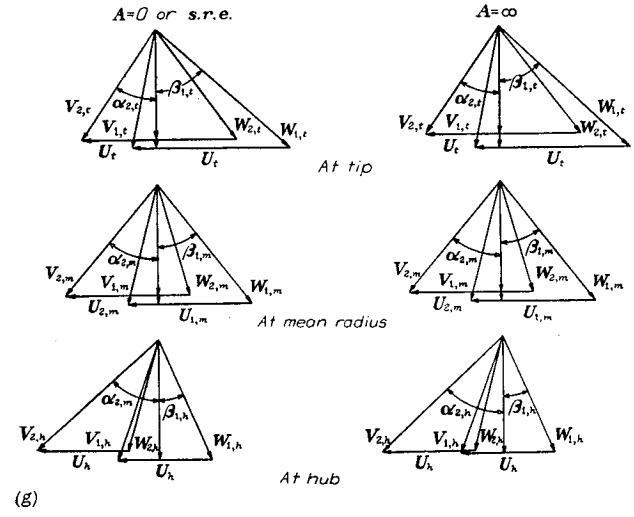

(g) Velocity diagrams at different radii.

FIGURE 5.—Concluded. Free-vortex and constant-total-enthalpy compressor.

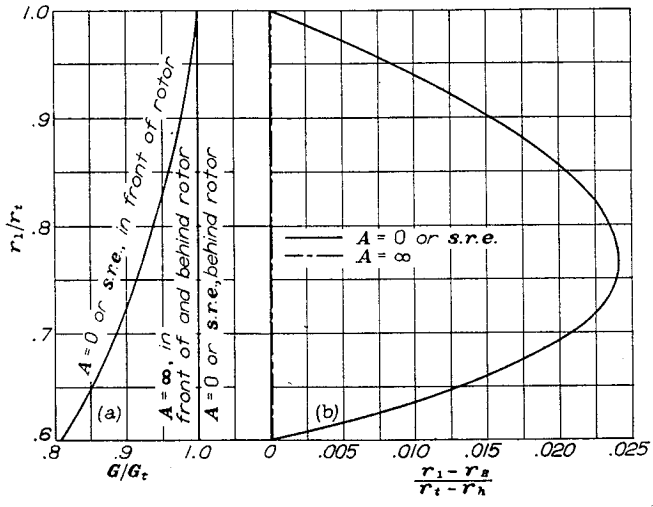

(a) Distribution of specific mass flow. (b) Radial displacement across rotor.

FIGURE 6.—Free-vortex and constant-total-enthalpy turbine.

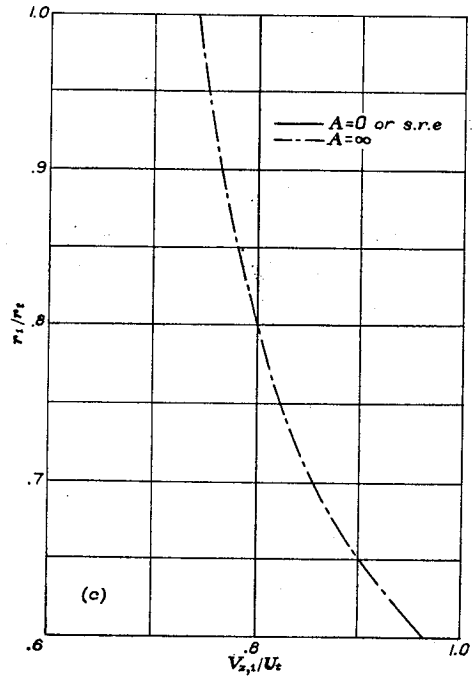

(c) Variation of axial velocity ahead of rotor.

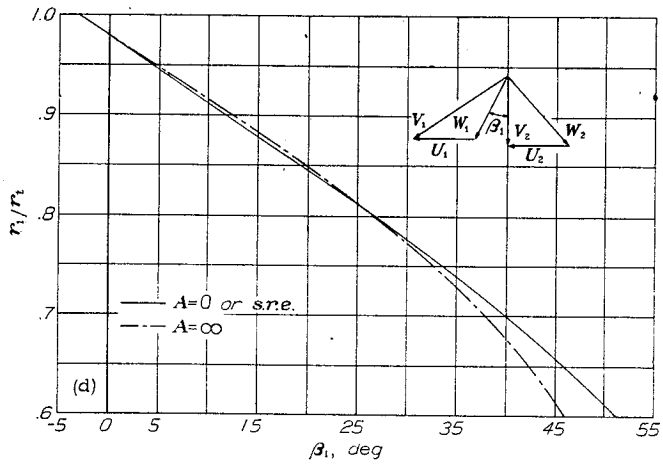

(d) Variation of gas angle entering rotor blades.

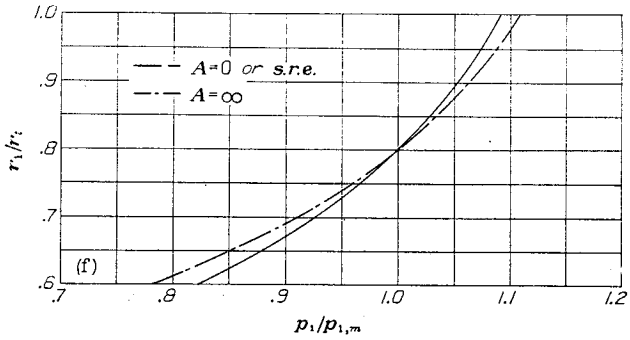

(f) Pressure distribution.

The variation of axial velocity ahead of the rotor is shown in figure 6(c). An increasing axial velocity toward the hub of about 15 percent would be required for an aspect ratio of 2.

Figure 6(d) shows the radial variation of gas angles entering rotor blades. The difference is only important at the hub. In the actual case of an aspect ratio of 2, the simplified calculation would give an angle of attack 3° to 4° too high at the hub.

The absolute and relative Mach numbers of gas ahead of the rotor are shown in figure 6(e). In the actual case of an aspect ratio of 2, the Mach number at the hub is about 3 percent higher than the simplified calculation.

Figure 6(f) shows the pressure distribution ahead of the rotor. For an aspect ratio of 2, the pressures at the tip and at the hub are about 2 percent higher and 3 percent lower than the simplified calculation, respectively.

The velocity diagrams at three radii for the zero and infinite aspect ratios are shown in figure 6(g).

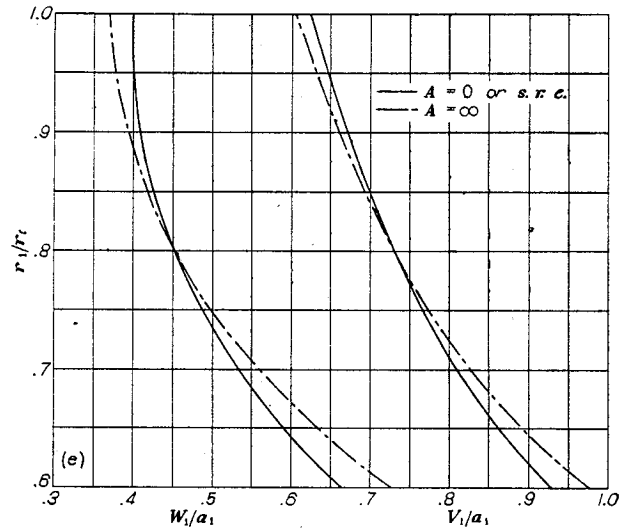

(e) Variation of Mach number ahead of rotor.

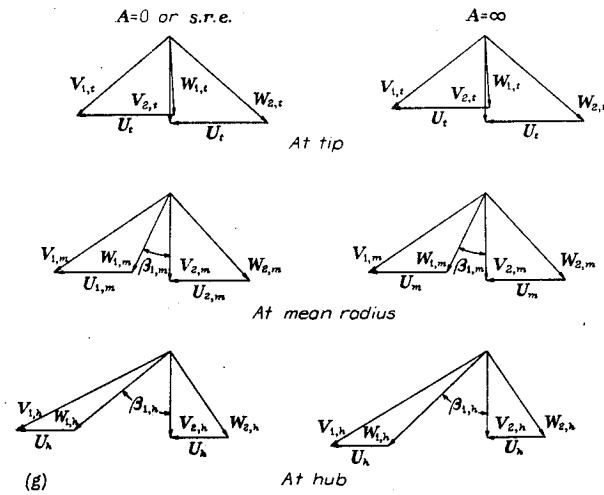

(g) Velocity diagrams at different radii.

FIGURE 6.—Concluded. Free-vortex and constant-total-enthalpy turbine.

SUMMARY OF ANALYSIS AND CALCULATIONS

In axial-flow turbomachines, radial motion of gas occurs because of the tapering of the passage walls and the variation of gas conditions across blade rows specified in the design. The direction and the magnitude of this radial flow depend on the type of design, the tapering of the passage walls, the blade-row aspect ratio, and the Mach number of gas flow. Even in the free-vortex type of design employing nontapered passage walls and requiring no change in velocity distributions from stage to stage, an appreciable amount of oscillatory radial motion occurs within the stage.

This radial motion gives an additional term to the ordinary radial-equilibrium equation. In the free space between blade rows, this additional term is approximately equal to the product of the square of axial velocity and the curvature caused by the radial flow. Depending on whether the curvature is positive or negative, the radial pressure gradient caused by the whirling motion of gas is decreased or increased, respectively, by this additional term.

The determination of this radial-flow path requires a long process of step-by-step calculation. It is found, however, that a sinusoidal radial-flow path gives an effect on the radial variation of gas condition between blade rows as small as possible without discontinuity in the curvature of the streamline. It may therefore be desirable to prescribe this simple radial-flow path in the design. Also, inasmuch as it represents the major harmonic of the radial-flow path that may exist in any design in which the blade loading is relatively uniform in the axial direction, the calculation based on this simple radial-flow path gives good approximate results.

Methods of solution for the limiting cases of zero and infinite blade aspect ratios and a simple approximate solution of the radial displacement across the blade row having a finite aspect ratio are also obtained.

The analysis made of the maximum compatible number of the degrees of freedom in specifying the radial variations of gas properties in stations between successive blade rows of a turbomachine shows that the designer is free to specify one such variation at each of the stations. The various ways to use up these degrees of freedom and the resultant types of design obtained are discussed.

The usual method of calculation, which neglects the radial motion, gives results close only to the case in which the axial length of the blade row is much larger than its radial length, and is not good for the case of a finite blade-row aspect ratio. The difference between the results obtained by the usual method and the method suggested herein is found to be quite large in a design employing constant total enthalpy and a symmetrical velocity diagram along the radii. Calculation made for this type of compressor, using the same limiting Mach number, same limiting turning, same axial velocity at the mean radius, and for a blade-row aspect ratio of 2, gives the following differences between the usual and the suggested method:

1. The radial variation of axial velocity ahead of the rotor is 13 percent for the usual method and 28 percent for the suggested method, and the radial variation of axial velocity behind the rotor is 53 percent for the usual method and 40 percent for the suggested method (all expressed in terms of their values at the mean radius).
2. The air angles differ from 1° to 3° at the hub and at the tip.
3. The radial variation of Mach number relative to the rotor blade in the usual method is 9 percent lower than that in the suggested method.
4. The radial variation in static-pressure rise across the rotor is 13 percent for the usual method and only 2 percent for the suggested method.
5. The mass flow in the usual method is 4 percent higher than that in the suggested method.
6. The allowable rotor speed in the usual method is 5 percent higher than that in the suggested method.

LEWIS FLIGHT PROPULSION LABORATORY,
NATIONAL ADVISORY COMMITTEE FOR AERONAUTICS,
CLEVELAND, OHIO, *January 1, 1949*.

APPENDIX A

SYMBOLS

The following symbols are used in this report:

A aspect ratio of blade row, $\frac{r_t-r_h}{L}$

a velocity of sound

C_L lift coefficient

c_p specific heat of gas at constant pressure

c_v specific heat of gas at constant volume

$\frac{D}{Dt}$ differentiation with respect to time following motion of gas

$\overline{F}$ external force per unit mass of gas (general case); circumferentially uniformly distributed blade force per unit mass of gas (axially symmetric case)

F_r radial component of $\overline{F}$

F_z axial component of $\overline{F}$

F_θ tangential component of $\overline{F}$

f form of radial-flow path

G mass flow per unit flow area perpendicular to axis of turbomachine

g form of radial-displacement distribution

H total enthalpy per unit of gas, $h+\frac{V^2}{2}$

h enthalpy per unit mass of gas, $u+\frac{p}{\rho}$

K constant

k thermal conductivity of gas

L axial length of blade row (fig. 3)

M Mach number of gas

m mass of gas

n polytropic exponent of actual expansion or compression process of gas

p static pressure

Q heat input to unit mass of gas along its path of motion per unit time from neighboring gas particles in general case or from blade and passage wall in axially symmetric case

R gas constant

r radial distance measured from axis of turbomachine

r_o mean radius of radial-flow path (fig. 3(a))

$r' = \frac{r}{r_t-r_h}$

s entropy per unit mass of gas

$s.r.e.$ simplified-radial-equilibrium approximation

T absolute stream temperature of gas

t time

U magnitude of $\overline{U}$

$\overline{U}$ vector velocity of blade at radius r

u internal energy per unit mass of gas with 0° absolute as base temperature

V magnitude of $\overline{V}$

$\overline{V}$ absolute vector velocity of gas

V_r radial component of $\overline{V}$

V_z axial component of $\overline{V}$

V_θ tangential component of $\overline{V}$

W magnitude of $\overline{W}$

$\overline{W}$ vector velocity of gas relative to rotor blade

W_θ tangential component of $\overline{W}$

y maximum radial displacement over blade height

z distance along axis of turbomachine

α angle between absolute velocity of gas and axis of turbomachine

β angle between relative velocity of gas and axis of turbomachine

γ ratio of specific heats, c_p/c_v

Δ radial displacement across rotor, r_2-r_1

δ dimensionless turning, $\frac{\zeta_2-\zeta_1}{r_1U_{1,t}}$

ζ angular momentum about z-axis per unit mass of gas, rV_θ

η small-stage or polytropic efficiency

θ angular coordinate measured from some fixed radial line

μ absolute viscosity of gas

ρ mass density of gas

σ blade solidity

Φ dissipation of energy due to viscosity per unit volume of gas per unit time

φ function

χ angular coordinate measured relative to rotor

ω angular velocity of blade

Subscripts:

1 ahead of rotor

2 behind rotor and ahead of stator

3 behind stator and ahead of next rotor

c satisfying continuity equation

e satisfying radial-equilibrium and total-enthalpy equations

h hub

i any station between two blade rows

j any station

k station short distance downstream of station j

l limiting value

m at mean radius

n used with r to indicate radius where maximum radial displacement occurs

s simplified-radial-equilibrium approximation

t tip

APPENDIX B

DERIVATION OF EQUATIONS

From equations (4), (7), and (9), and the relations

$$R=c_p-c_v \tag{B1}$$

and

$$\gamma=\frac{c_p}{c_v} \tag{B2}$$

there is obtained

$$dh=\frac{\gamma}{\gamma-1}\,d\left(\frac{p}{\rho}\right) \tag{B3}$$

From equations (8) and (B3),

$$dH=\frac{\gamma}{\gamma-1}\,d\left(\frac{p}{\rho}\right)+d\left(\frac{V^2}{2}\right) \tag{B4}$$

From equations (9) and (10),

$$T\,ds=dh-\frac{dp}{\rho} \tag{B5}$$

By use of equation (B3),

$$T\,ds=\frac{\gamma}{\gamma-1}\,d\left(\frac{p}{\rho}\right)-\frac{dp}{\rho} \tag{B6}$$

By use of equation (7),

$$d\left(\frac{s}{R}\right)=\frac{1}{\gamma-1}\frac{dp}{p}-\frac{\gamma}{\gamma-1}\frac{d\rho}{\rho} \tag{B7}$$

$$=\frac{1}{\gamma-1}\,d\left(\log_e\frac{p}{\rho^\gamma}\right) \tag{B8}$$

$$=\frac{1}{\gamma-1}\,d\left(\log_e\frac{p}{\rho}\right)-d\,(\log_e\rho) \tag{B9}$$

$$=\frac{1}{\gamma-1}\,d\,(\log_e T)-d\,(\log_e\rho) \tag{B10}$$

Equation (1) may be written as

$$\nabla\cdot\overline{V}+\frac{D}{Dt}\log_e\rho=0$$

Combining with equation (B10) yields the following form of the continuity relation:

$$\nabla\cdot\overline{V}+\frac{1}{\gamma-1}\frac{D}{Dt}\log_e T-\frac{D}{Dt}\left(\frac{s}{R}\right)=0 \tag{1a}$$

From equation (2) and the following relations

$$\frac{D\overline{V}}{Dt}=\frac{\partial\overline{V}}{\partial t}+(\overline{V}\cdot\nabla)\,\overline{V}$$

and

$$(\overline{V}\cdot\nabla)\,\overline{V}=\frac{1}{2}\nabla V^2-\overline{V}\times(\nabla\times\overline{V})$$

there is obtained

$$\frac{\partial\overline{V}}{\partial t}-\overline{V}\times(\nabla\times\overline{V})+\frac{1}{2}\nabla V^2=\overline{F}-\frac{1}{\rho}\nabla p+\frac{\mu}{\rho}\left[\nabla^2\overline{V}+\frac{1}{3}\nabla(\nabla\cdot\overline{V})\right]+$$
$$\frac{1}{\rho}\left\{2\,[(\nabla\mu)\cdot\nabla]\,\overline{V}+(\nabla\mu)\times(\nabla\times\overline{V})-\frac{2}{3}\,(\nabla\cdot\overline{V})\,(\nabla\mu)\right\} \tag{B11}$$

From equations (B4) and (B6),

$$\frac{1}{2}\nabla V^2+\frac{1}{\rho}\nabla p=\nabla H-\frac{\gamma}{\gamma-1}\nabla\left(\frac{p}{\rho}\right)+\frac{1}{\rho}\nabla p$$
$$=\nabla H-T\nabla s$$

Combining with equation (B11) yields

$$\nabla H=\overline{F}+T\nabla s+\overline{V}\times(\nabla\times\overline{V})-\frac{\partial\overline{V}}{\partial t}+\frac{\mu}{\rho}\left[\nabla^2\overline{V}+\frac{1}{3}\nabla(\nabla\cdot\overline{V})\right]+$$
$$\frac{1}{\rho}\left\{2\,[(\nabla\mu)\cdot\nabla]\,\overline{V}+(\nabla\mu)\times(\nabla\times\overline{V})-\frac{2}{3}\,(\nabla\cdot\overline{V})\,(\nabla\mu)\right\}$$

From equations (8) and (B5),

$$\frac{DH}{Dt}=T\frac{Ds}{Dt}+\frac{1}{\rho}\frac{Dp}{Dt}+\overline{V}\cdot\frac{D\overline{V}}{Dt}$$
$$=T\frac{Ds}{Dt}+\frac{1}{\rho}\frac{\partial p}{\partial t}+\overline{V}\cdot\left(\frac{1}{\rho}\nabla p+\frac{D\overline{V}}{Dt}\right)$$

By combining with equation (2),

$$\frac{DH}{Dt}=T\frac{Ds}{Dt}+\frac{1}{\rho}\frac{\partial p}{\partial t}+\overline{V}\cdot\left(\overline{F}+\frac{\mu}{\rho}\left[\nabla^2\overline{V}+\frac{1}{3}\nabla(\nabla\cdot\overline{V})\right]+\right.$$
$$\left.\frac{1}{\rho}\left\{2\,[(\nabla\mu)\cdot\nabla]\,\overline{V}+(\nabla\mu)\times(\nabla\times\overline{V})-\frac{2}{3}\,(\nabla\cdot\overline{V})\,(\nabla\mu)\right\}\right)$$

When combined with equations (3) and (10),

$$\frac{DH}{Dt}=Q+\frac{\Phi}{\rho}+\frac{1}{\rho}\frac{\partial p}{\partial t}+\overline{V}\cdot\left(\overline{F}+\frac{\mu}{\rho}\left[\nabla^2\overline{V}+\frac{1}{3}\nabla(\nabla\cdot\overline{V})\right]+\right.$$
$$\left.\frac{1}{\rho}\left\{2\,[(\nabla\mu)\cdot\nabla]\,\overline{V}+(\nabla\mu)\times(\nabla\times\overline{V})-\frac{2}{3}\,(\nabla\cdot\overline{V})\,(\nabla\mu)\right\}\right) \tag{3a}$$

From equations (3) and (10),

$$T\frac{Ds}{Dt}=Q+\frac{\Phi}{\rho}$$

or

$$\frac{Ds}{Dt}=\frac{Q}{T}+R\frac{\Phi}{p} \tag{3b}$$

For steady axially symmetric flow of nonviscous fluid, equation (3a) reduces to

$$\frac{DH}{Dt}=Q+\overline{F}\cdot\overline{V} \tag{B12}$$

From equation (11),

$$\overline{F}\cdot\overline{V}=\overline{F}\cdot\overline{U}$$
$$=F_\theta U$$
$$=rF_\theta\omega \tag{B13}$$

From equation (15),

$$rF_\theta = V_r \frac{\partial(rV_\theta)}{\partial r} + V_z \frac{\partial(rV_\theta)}{\partial z}$$

$$= \frac{D(rV_\theta)}{Dt} \tag{B14}$$

Combining equations (B12), (B13), and (B14) yields

$$\frac{DH}{Dt} = Q + \omega \frac{D(rV_\theta)}{Dt} \tag{18}$$

For steady axially symmetric flow of a viscous fluid, equation (18) is obtained by applying motion and energy equations to a mass system with a fixed control surface, as shown by the solid lines in figure 2. Under steady axially symmetric flow, the mass inflow dm_j in time dt is equal to the mass outflow dm_k in time dt, the state of gas within the control surface is unchanged, and the state of gas at stations j and k is constant with respect to θ. By equation (B11), the sum of the tangential blade force and the tangential viscous gas forces exerted by the surrounding gas particles on the system is equal to

$$\frac{1}{r} \frac{D(rV_\theta)}{Dt} dm_j$$

The torque about the z-axis exerted by these tangential forces on mass dm_j is therefore simply $\frac{D(rV_\theta)}{Dt} dm_j$ and the work input to mass dm_j by these tangential forces in time dt is equal to

$$\frac{D(rV_\theta)}{Dt} dm_j \, \omega \, dt = \omega[(rV_\theta)_k - (rV_\theta)_j] dm_j$$

In passing from station j to station k, in addition to receiving this work input, the gas particles are doing work against the axial and radial viscous forces exerted by the surrounding gas particles. This negative work is usually small, however; if it is assumed that the heat generated by the frictional work is added back to the same gas stream, the heat addition cancels the negative work, and the energy equation for steady flow gives

$$(H_k - H_j) dm_j = \int_{t_j}^{t_k} Q \, dm_j \, dt + \omega[(rV_\theta)_k - (rV_\theta)_j] dm_j$$

or

$$\frac{DH}{Dt} = Q + \omega \frac{D(rV_\theta)}{Dt} \tag{18}$$

where Q denotes the rate per unit mass at which the gas stream sheet is receiving heat from external source through blades or other passage walls.

When equation (19) is given, the entropy change can be obtained in the following manner: From equation (B10),

$$\frac{D}{Dt}\left(\frac{s}{R}\right) = \frac{1}{\gamma - 1} \frac{D}{Dt} \log_e T - \frac{D}{Dt} \log_e \rho \tag{B15}$$

But by equations (19) and (7),

$$\frac{D}{Dt} \log_e \rho = \frac{1}{n-1} \frac{D}{Dt} \log_e T$$

Substituting into equation (B15) gives

$$\frac{Ds}{Dt} = R\left(\frac{1}{\gamma - 1} - \frac{1}{n-1}\right) \frac{D}{Dt} \log_e T$$

$$= R \frac{n-\gamma}{(n-1)(\gamma-1)} \frac{D}{Dt} \log_e T \tag{B16}$$

For steady axially symmetric flow, equation (B16) reduces to

$$\frac{Ds}{Dt} = R \frac{n-\gamma}{(n-1)(\gamma-1)} \left(V_r \frac{\partial}{\partial r} \log_e T + V_z \frac{\partial}{\partial z} \log_e T\right) \tag{20}$$

For successive axial stations j and k a short distance apart, equation (B16) gives

$$s_k(r_k) - s_j(r_j) = R \frac{n-\gamma}{(n-1)(\gamma-1)} [\log_e T_k(r_k) - \log_e T_j(r_j)]$$

$$= R \frac{n-\gamma}{(n-1)(\gamma-1)} \log_e \frac{T_k(r_k)}{T_j(r_j)} \tag{B17}$$

Inasmuch as the temperature change between the two successive stations is small, if the enthalpy is measured with 0° absolute as the base temperature, the temperature ratio can be considered equal to the enthalpy ratio:

$$\frac{T_k}{T_j} = \frac{h_k}{h_j} = \frac{H_k - \frac{V_k^2}{2}}{H_j - \frac{V_j^2}{2}} \tag{B18}$$

Substituting equation (B18) into equation (B17) gives

$$s_k(r_k) - s_j(r_j) = R \frac{n-\gamma}{(n-1)(\gamma-1)} \log_e \frac{H_k - \frac{V_k^2}{2}}{H_j - \frac{V_j^2}{2}} \tag{20a}$$

The density ratio between the two stations is obtained from equation (B10)

$$\frac{\rho_k}{\rho_j} = \left(\frac{T_k}{T_j}\right)^{\frac{1}{\gamma-1}} e^{-\frac{s_k - s_j}{R}} \tag{B19}$$

Combining with equation (B18) yields

$$\frac{\rho_k}{\rho_j} = \left(\frac{H_k - \frac{V_k^2}{2}}{H_j - \frac{V_j^2}{2}}\right)^{\frac{1}{\gamma-1}} e^{-\frac{s_k - s_j}{R}} \tag{B20}$$

Substituting into equation (22) gives

$$V_{z,k}\left(H_k - \frac{V_k^2}{2}\right)^{\frac{1}{\gamma-1}} e^{-\frac{s_k}{R}} r_k \, dr_k = V_{z,j}\left(H_j - \frac{V_j^2}{2}\right)^{\frac{1}{\gamma-1}} e^{-\frac{s_j}{R}} r_j \, dr_j \tag{22a}$$

APPENDIX C

DETERMINATION OF RADIAL DISPLACEMENT BY USE OF CONTINUITY EQUATION

Equation (22) may be written as a linear differential equation for r_2^2 as a function of r_1, provided $G_2(r_1)$ is known:

$$\frac{d(r_2^2)}{dr_1}=2\frac{G_1(r_1)}{G_2(r_1)}r_1$$

$$r_2^2=-\int_{r_1}^{r_{1,t}}\frac{G_1(r_1)}{G_2(r_1)}2r_1\,dr_1+r_{2,t}^2 \qquad \text{(C1)}$$

when divided by $r_{2,t}^2$,

$$\left(\frac{r_2}{r_{2,t}}\right)^2=1-\left(\frac{r_{1,t}}{r_{2,t}}\right)^2\int_{r_1}^{r_{1,t}}\frac{G_1(r_1)}{G_2(r_1)}\,2\,\frac{r_1}{r_{1,t}}\,\frac{dr_1}{r_{1,t}} \qquad \text{(C2)}$$

If G_1 and G_2 are unknown and only $G_1/G_{1,t}$ and $G_2/G_{2,t}$ are known, a modification is necessary:

$$\left(\frac{r_2}{r_{2,t}}\right)^2=1-\left(\frac{r_{1,2}}{r_{2,t}}\right)^2\frac{G_{1,t}}{G_{2,t}}\int_{r_1}^{r_{1,t}}\frac{\dfrac{G_1}{G_{1,t}}(r_1)}{\dfrac{G_2}{G_{2,t}}(r_1)}\,2\,\frac{r_1}{r_{1,t}}\,\frac{dr_1}{r_{1,t}} \qquad \text{(C3)}$$

The value of $G_{1,t}/G_{2,t}$ is found by the condition that total mass flow at stations 1 and 2 is the same:

$$\left(\frac{r_{1,t}}{r_{2,t}}\right)^2\frac{G_{1,t}}{G_{2,t}}=\frac{1-\left(\dfrac{r_{2,h}}{r_{2,t}}\right)^2}{\displaystyle\int_{r_{1,h}}^{r_{1,t}}\frac{\dfrac{G_1}{G_{1,t}}(r_1)}{\dfrac{G_2}{G_{2,t}}(r_1)}\,2\,\frac{r_1}{r_{1,t}}\,\frac{dr_1}{r_{1,t}}} \qquad \text{(C4)}$$

Hence

$$\left(\frac{r_2}{r_{2,t}}\right)^2=1-\left[1-\left(\frac{r_{2,h}}{r_{2,t}}\right)^2\right]\frac{\displaystyle\int_{r_1}^{r_{1,t}}\frac{\dfrac{G_1}{G_{1,t}}(r_1)}{\dfrac{G_2}{G_{2,t}}(r_1)}\,\frac{r_1}{r_{1,t}}\,\frac{dr_1}{r_{1,t}}}{\displaystyle\int_{r_{1,h}}^{r_{1,t}}\frac{\dfrac{G_1}{G_{1,t}}(r_1)}{\dfrac{G_2}{G_{2,t}}(r_1)}\,\frac{r_1}{r_{1,t}}\,\frac{dr_1}{r_{1,t}}} \qquad \text{(C5)}$$

APPENDIX D

EQUATIONS FOR SIMPLIFIED-RADIAL-EQUILIBRIUM CALCULATIONS

Equations to calculate distributions of gas properties at three stations of a typical stage under the simplified-radial-equilibrium approximation for a few types of design are given.

GROUP I

Free vortex.—For this design,

$$\frac{d\zeta_t}{dr_t}=0 \qquad \text{(D1)}$$

When the inlet total enthalpy is constant with respect to r and the radial variation of entropy is negligible, equation (14g) reduces to

$$\frac{dV_{z,t}}{dr_t}=0 \qquad \text{(D2)}$$

The variation in tangential velocity is, by equation (D1),

$$V_{\theta,t}=V_{\theta,t,t}\,\frac{r_{t,t}}{r_t} \qquad \text{(D3)}$$

At each station, by using equations (30) and (D3),

$$\gamma\,\frac{p_t}{\rho_t^{\gamma}}\,\rho^{\gamma-2}\,\frac{\partial\rho}{\partial r}=\frac{(V_{\theta,t}r_t)^2}{r^3}$$

When the preceding equation is integrated from r to r_t, and the relation

$$a=\sqrt{\frac{\gamma p}{\rho}}$$

is used, there is obtained

$$\frac{\rho}{\rho_t}=\left\{1-\frac{\gamma-1}{2}\left(\frac{V_{\theta,t}}{a_t}\right)^2\left[\left(\frac{r_t}{r}\right)^2-1\right]\right\}^{\frac{1}{\gamma-1}} \qquad \text{(D4)}$$

This equation holds for all stations, provided the appropriate values of $(V_{\theta,t}/a_t)$ are used. It follows from equation (D2) that at each station

$$\frac{G}{G_t}=\frac{\rho}{\rho_t} \qquad \text{(D5)}$$

The radial position of gas at station 2 or 3 can be obtained by numerically integrating equation (C5) using distributions of specific mass flow given by equation (D5). An alternate method is to expand the right side of equation (D4) into a binominal series. Because $\frac{\gamma-1}{2}\left(\frac{V_{\theta,t}}{a_t}\right)^2\left[\left(\frac{r_t}{r}\right)^2-1\right]$ is usually less than 0.15, three terms will be sufficient. Let $\bar{\rho}_r$ represent the average density in the annulus between r and r_t, then

$$\frac{\bar{\rho}_r}{\rho_t}=\frac{\displaystyle\int_r^{r_t}2\pi\rho r\,dr}{\pi(r_t^2-r^2)\rho_t}$$

$$=1+\frac{1}{2}\left(\frac{V_{\theta,t}}{a_t}\right)^2+\frac{2-\gamma}{8}\left(\frac{V_{\theta,t}}{a_t}\right)^4+\left[\frac{1}{2}\left(\frac{V_{\theta,t}}{a_t}\right)^2+\frac{2-\gamma}{4}\left(\frac{V_{\theta,t}}{a_t}\right)^4\right]\frac{\log_e\left(\dfrac{r}{r_t}\right)^2}{1-\left(\dfrac{r}{r_t}\right)^2}+\frac{2-\gamma}{8}\left(\frac{V_{\theta,t}}{U_t}\right)^4\left(\frac{r_t}{r}\right)^2+\ldots \qquad \text{(D6)}$$

and inasmuch as

$$\bar{\rho}_{r,1}V_{z,1}(r_{1,t}^2-r_1^2)=\bar{\rho}_{r,2}V_{z,2}(r_{2,t}^2-r_2^2)$$

or

$$\frac{\bar{\rho}_{r,1}(r_{1,t}^2-r_1^2)}{\bar{\rho}_{r,2}(r_{2,t}^2-r_2^2)}=\frac{V_{z,2}}{V_{z,1}}=\frac{\bar{\rho}_{h,1}(r_{1,t}^2-r_{1,h}^2)}{\bar{\rho}_{h,2}(r_{2,t}^2-r_{2,h}^2)}$$

$$\left(\frac{r_2}{r_{2,t}}\right)^2=1-\left[\frac{1-\left(\frac{r_{2,h}}{r_{2,t}}\right)^2}{1-\left(\frac{r_{1,h}}{r_{1,t}}\right)^2}\right]\left[1-\left(\frac{r_1}{r_{1,t}}\right)^2\right]\frac{\frac{\bar{\rho}_{r,1}}{\bar{\rho}_{h,1}}}{\frac{\bar{\rho}_{r,2}}{\bar{\rho}_{h,2}}} \qquad \text{(D7)}$$

The change of total enthalpy across the rotor is

$$H_2-H_1=\omega(\zeta_2-\zeta_1)$$

Then

$$\frac{H_2}{H_1}=1+\frac{\omega(\zeta_2-\zeta_1)}{H_1}$$

For compressor,

$$\frac{H_2}{H_1}=1+\frac{r_{1,h}}{r_{1,t}}\frac{V_{z,1,h}}{U_{1,t}}\frac{\frac{r_{2,h}}{r_{1,h}}V_{\theta,2,h}-V_{\theta,1,h}}{V_{z,1,h}}\frac{U_{1,t}^2}{H_1}$$

where

the quantity $\dfrac{\frac{r_{2,h}}{r_{1,h}}V_{\theta,2,h}-V_{\theta,1,h}}{V_{z,1,h}}$ is to be chosen by the designer.

Inasmuch as

$$H_1=h_{1,t}+\frac{V_{1,t}^2}{2}$$

$$=\frac{a_{1,t}^2}{\gamma-1}+\frac{1}{2}(V_{z,1,t}^2+V_{\theta,1,t}^2)$$

and

$$a_{1,t}^2=\left(\frac{W_{1,t}}{M_t}\right)^2$$

$$=\frac{1}{M_t^2}[V_{z,1,t}^2+(U_{1,t}^2-V_{\theta,1,t})^2]$$

where M_t is the limiting Mach number to be chosen by the designer,

---

$$\frac{H_2}{H_1}=1+\frac{\frac{r_{1,h}}{r_{1,t}}\frac{V_{z,1,h}}{U_{1,t}}\frac{\frac{r_{2,h}}{r_{1,h}}V_{\theta,2,h}-V_{\theta,1,h}}{V_{z,1,h}}}{\frac{1}{(\gamma-1)M_t^2}\left[\left(\frac{V_{z,1,t}}{U_{1,t}}\right)^2+\left(1-\frac{V_{\theta,1,t}}{U_{1,t}}\right)^2\right]+\frac{1}{2}\left[\left(\frac{V_{z,1,t}}{U_{1,t}}\right)^2+\left(\frac{V_{\theta,1,t}}{U_{1,t}}\right)^2\right]} \qquad \text{(D8)}$$

The pressure distribution at each station is obtained by raising its density distribution (equation (D4)) to the power γ. The pressure changes between the stations at different radii are obtained by combining these pressure distributions with the pressure change across the rotor at the radius where the value of the polytropic exponent is known or assumed. The angle that the gas velocity makes with the axis of the machine at any radius is obtained from the known tangential and axial velocities.

Symmetrical velocity diagram.—For the nontapered passage, $r_1=r_2=r$ and from equations (39) and (42a)

$$\left.\begin{aligned}\frac{d\zeta_1}{dr}&=\frac{d\zeta_2}{dr}=\omega r\\ \zeta_1&=\frac{\omega r^2}{2}-\frac{r_{1,t}\delta_t U_{1,t}}{2}\\ \zeta_2&=\frac{\omega r^2}{2}+\frac{r_{1,t}\delta_t U_{1,t}}{2}\end{aligned}\right\} \qquad \text{(D9)}$$

or

$$\left.\begin{aligned}\frac{V_{\theta,1}}{U_{1,t}}&=\frac{1}{2}\frac{r}{r_{1,t}}-\frac{\delta_t}{2}\frac{r_{1,t}}{r}\\ \frac{V_{\theta,2}}{U_{1,t}}&=\frac{1}{2}\frac{r}{r_{1,t}}+\frac{\delta_t}{2}\frac{r_{1,t}}{r}\end{aligned}\right\} \qquad \text{(D10)}$$

When equation (D10) is substituted into equation (30),

$$\gamma\frac{p_h}{\rho_h^\gamma}\rho^{\gamma-2}\frac{\partial\rho}{\partial r}=\frac{\omega^2 r}{4}\mp\frac{\delta_t U_{1,t}^2}{2r}+\frac{1}{4}(r_{1,t}\delta_t U_{1,t})^2\frac{1}{r^3}$$

where the minus sign is used for station 1 and the plus sign for station 2. Inetgration from r_h to r yields

$$\frac{\rho}{\rho_h}=\left\{1+\frac{\gamma-1}{8}\frac{U_t^2}{a_h^2}\left[\left(\frac{r}{r_t}\right)^2-\left(\frac{r_h}{r_t}\right)^2\mp 4\delta_t\left(\frac{U_{1,t}}{U_t}\right)^2\log_e\frac{r}{r_h}+\delta_t^2\left(\frac{U_{1,t}}{U_t}\right)^2\left(\frac{r_t^2}{r_h^2}-\frac{r_t^2}{r^3}\right)\right]\right\}^{\frac{1}{\gamma-1}} \qquad \text{(D11)}$$

where the minus sign is used for station 1 and the plus sign for station 2.

For the case where the inlet total enthalpy is constant with respect to radius and the radial variation of entropy is negligible, the variation of axial velocity is obtained from equation (14g):

$$V_z\frac{dV_z}{dr}=-\frac{1}{r^2}\zeta\frac{d\zeta}{dr}$$

$$=-U_{1,t}^2\left(\frac{r}{2r_{1,t}^2}\pm\frac{\delta_t}{2r}\right) \qquad \text{(D12)}$$

Integration from r_h to r gives

$$\left(\frac{V_z}{U_{1,t}}\right)^2=\left(\frac{V_{z,h}}{U_{1,t}}\right)^2-\frac{1}{2}\left(\frac{r^2}{r_{1,t}^2}-\frac{r_h^2}{r_{1,t}^2}\right)\pm\delta_t\log_e\frac{r}{r_h} \qquad \text{(D13)}$$

where the plus sign in the last term is used for station 1 and the minus sign for station 2.

When both V_θ and V_z are known, the radial variation of density can also be obtained by applying equation (B20) at the station:

$$\frac{\rho}{\rho_h}=\left[\frac{H-\frac{1}{2}(V_\theta^2+V_z^2)}{H-\frac{1}{2}(V_{\theta,h}^2+V_{z,h}^2)}\right]^{\frac{1}{\gamma-1}} \tag{D14}$$

In the tapered passage, the gas is assumed to flow in conical surfaces, which gives the value of r_2 as a function of r_1. Equations (39) and (43) give the distributions of ζ and V_θ as shown by equations (E5) and (E6), respectively, given in appendix E. The distribution of axial velocity at station 2 is the same as that given by equation (E8). The density distributions can be obtained from equation (D14). After these distributions are known, the distribution of specific mass flow G is known and the radial displacement is found by using equation (C5).

In compressors of this design, the maximum value of $\frac{\frac{r_{2,h}}{r_{1,h}}V_{\theta,2}-V_{\theta,1}}{V_{z,1}}$ is usually at the hub. Its value there is to be set by the designer. Then

$$\delta_h=\frac{\zeta_{2,h}-\zeta_{1,h}}{r_{1,h}}\frac{}{U_{1,t}}=\frac{\frac{r_{2,h}}{r_{1,h}}V_{\theta,2,h}-V_{\theta,1,h}}{V_{z,1,h}}\frac{V_{z,1,h}}{U_{1,t}}$$

and

$$\delta_t=\frac{r_{1,h}}{r_{1,t}}\delta_h=\frac{r_{1,h}}{r_{1,t}}\frac{V_{z,1,h}}{U_{1,t}}\frac{\frac{r_{2,h}}{r_{1,h}}V_{\theta,2,h}-V_{\theta,1,h}}{V_{z,1,h}} \tag{D15}$$

In this type of design, the limiting Mach number is usually at the hub. Hence the denominator of the last term of equation (D8) should be replaced by

$$\frac{1}{(\gamma-1)M_t^2}\left[\left(\frac{V_{z,1,h}}{U_{1,t}}\right)^2+\left(\frac{U_{1,h}-V_{\theta,1,h}}{U_{1,t}}\right)^2\right]+\frac{1}{2}\left[\left(\frac{V_{z,1,h}}{U_{1,t}}\right)^2+\left(\frac{V_{\theta,1,h}}{U_{1,t}}\right)^2\right]$$

The rest of the calculation is the same as in the previous design.

Wheel-type tangential velocity in front of rotor.—When the case of constant total enthalpy is again considered at the inlet and the radial variation in entropy is neglected, with

$$V_{\theta,1}=K_1r_1=V_{\theta,1,t}\frac{r_1}{r_{1,t}} \tag{D16}$$

equation (14g) gives

$$\frac{dV_{z,1}^2}{dr_1}=-4K_1^2r_1$$

Integrating from hub to radius r yields

$$V_{z,1}^2=V_{z,1,h}^2-2K_1^2(r_1^2-r_{1,h}^2)$$

or

$$\left(\frac{V_{z,1}}{U_{1,t}}\right)^2=\left(\frac{V_{z,1,h}}{U_{1,t}}\right)^2-2\left(\frac{V_{\theta,1,t}}{U_{1,t}}\right)^2\left[\left(\frac{r_1}{r_{1,t}}\right)^2-\left(\frac{r_{1,h}}{r_{1,t}}\right)^2\right] \tag{D17}$$

With radially constant work input to the rotor, and a non-tapered passage,

$$r_2V_{\theta,2}=K_1r_1^2+\delta_tr_{1,t}U_{1,t} \tag{D18}$$

and

$$\left(\frac{V_{z,2}}{U_{1,t}}\right)^2=\left(\frac{V_{z,2,h}}{U_{1,t}}\right)^2-2\left(\frac{V_{\theta,1,t}}{U_{1,t}}\right)^2\left[\left(\frac{r_1}{r_{1,t}}\right)^2-\left(\frac{r_{1,h}}{r_{1,t}}\right)^2\right]-4\frac{V_{\theta,1,t}}{U_{1,t}}\delta_t\log_e\frac{r_1}{r_{1,h}} \tag{D19}$$

Equations (D17) and (D18) show that the axial velocity rapidly decreases with radius at stations 1 and 2. If K_1 in equation (D16) is chosen to be $\omega/2$, the difference between this type of design and the previous one is very small.

GROUP II

Untwisted rotor blade.—Equation (52) gives

$$\frac{V_{\theta,i}-\omega r_i}{V_{z,1}}=\tan\beta_i=K_i \tag{D20}$$

where $i=1, 2$. When equations (14g) and (D20) are used, the following relation is obtained:

$$\left[\left(1+\frac{1}{K_i^2}\right)V_{\theta,i}-\frac{\omega r_i}{K_i^2}\right]\frac{dV_{\theta,i}}{dr_i}+\frac{V_{\theta,i}^2}{r_i}-\frac{\omega V_{\theta,i}}{K_i^2}=\frac{dH_i}{dr_i}-T_i\frac{ds_i}{dr_i}-\frac{\omega^2r_i}{K_i^2} \tag{D21}$$

or

$$[(1+K_i^2)V_{z,i}+K_i\omega r_i]\frac{dV_{z,i}}{dr_i}+\frac{K_i^2}{r_i}V_{z,i}^2+3K_i\omega V_{z,i}=\frac{dH_i}{dr_i}-T_i\frac{ds_i}{dr_i}-2\omega^2r_i \tag{D22}$$

Either equation (D21) or (D22) can be solved by a standard method of numerical integration. Equation (D20) is then used to find the remaining velocity component. In equations (D21) and (D22), dH_i/dr_i in later stations, except at the station ahead of first rotor, is, in general, not equal to zero even if it is equal to zero at the inlet. These ratios are to be determined by using equation (18b). The term containing entropy in the equations may be significant in the case of cooled turbine.

APPENDIX E

EQUATIONS FOR ZERO- AND INFINITE-ASPECT-RATIO CALCULATIONS

The method of calculations is given for the two types of design used in the numerical examples.

FREE VORTEX

Zero aspect ratio.—In this type of design, the zero-aspect-ratio case is the same as that of the simplified-radial-equilibrium approximation.

Infinite aspect ratio.—By equations (31) and (B20),

$$\frac{V_{z,2}}{V_{z,1}}=\frac{\rho_1}{\rho_2}=e^{\frac{s_2-s_1}{R}}\left(\frac{H_1-\frac{V_1^2}{2}}{H_2-\frac{V_2^2}{2}}\right)^{\frac{1}{\gamma-1}}\left(\frac{V_{z,2}}{V_{z,1}}e^{\frac{s_1-s_2}{R}}\right)^{\gamma-1}$$

$$=\frac{2H_1-(V_{\theta,1}^2+V_{z,1}^2)}{2H_2-(V_{\theta,2}^2+V_{z,2}^2)} \tag{E1}$$

An additional relation between $V_{z,1}$ and $V_{z,2}$ is necessary in order to solve the equation. In the section **Limiting case of infinite aspect ratio,** two equations are suggested. For this design, equation (33) gives

$$\frac{dV_{z,1}}{dr}+\frac{dV_{z,2}}{dr}=0$$

or

$$V_{z,1}+V_{z,2}=\text{constant} \tag{E2}$$

and equation (34) gives

$$V_{z,1}\frac{dV_{z,1}}{dr}+V_{z,2}\frac{dV_{z,2}}{dr}=0$$

or

$$V_{z,1}^2+V_{z,2}^2=\text{constant} \tag{E3}$$

Also from equations (F4) and (F5), when the square term in Δ_e is neglected

$$V_{z,1}V_{z,2}=\text{constant} \tag{E4}$$

The three preceding equations give practically the same results.

A convenient procedure of calculation is as follows:

(1) In order to compare the result with other cases, the same value of $V_{z,1,m}$ may be used. From equation (E1), $V_{z,2,m}$ is determined.

(2) Insert these values in equation (E2), (E3), or (E4) to obtain the constant in the equation.

(3) Assume a number of values of $V_{z,1}$; obtain $V_{z,2}$ by the same equation. Then use the following equation, which is obtained from equations (E1) and (D3), to solve for r/r_t:

$$\left(\frac{r}{r_t}\right)^2=\frac{(V_{\theta,2,t})^2-\left(e^{\frac{s_2-s_1}{R}}\frac{V_{z,1}}{V_{z,2}}\right)^{\gamma-1}(V_{\theta,1,t})^2}{2H_1\left[\frac{H_2}{H_1}-\left(e^{\frac{s_2-s_1}{R}}\frac{V_{z,1}}{V_{z,2}}\right)^{\gamma-1}\right]+\left(e^{\frac{s_2-s_1}{R}}\frac{V_{z,1}}{V_{z,2}}\right)^{\gamma-1}(V_{z,1})^2-(V_{z,2})^2}$$

(4) Plot $V_{z,1}$ and $V_{z,2}$ against r/r_t, and obtain $V_{z,1}$ and $V_{z,2}$ at the values of r/r_t desired.

When the distribution of axial velocity is known, the density variation at any station is obtained from equation (D14). The pressure variation at each station is obtained by raising the density ratio to the γ power. The pressure changes across the stage at different radii and the air angles are obtained in the same manner as in the simplified-radial-equilibrium calculation.

SYMMETRICAL VELOCITY DIAGRAM

Zero aspect ratio.—With radial displacement not equal to zero, the equations for tangential velocities are different from the expressions of equation (D10). From equations (39) and (43)

$$\frac{d\zeta_1}{dr_1}=\frac{d\zeta_2}{dr_1}=\omega r_1$$

$$\left.\begin{aligned}\zeta_1&=\frac{\omega r_1^2}{2}-\frac{r_{1,t}\delta_t U_{1,t}}{2}\\ \zeta_2&=\frac{\omega r_1^2}{2}+\frac{r_{1,t}\delta_t U_{1,t}}{2}\end{aligned}\right\} \tag{E5}$$

and

$$\left.\begin{aligned}\frac{V_{\theta,1}}{U_{1,t}}&=\frac{\zeta_1}{r_1U_{1,t}}=\frac{r_1}{2r_{1,t}}-\frac{r_{1,t}\delta_t}{2r_1}\\ \frac{V_{\theta,2}}{U_{1,t}}&=\frac{\zeta_2}{r_2U_{1,t}}=\left(\frac{r_1}{2r_{1,t}}+\frac{r_{1,t}\delta_t}{2r_1}\right)\frac{r_1}{r_2}\end{aligned}\right\} \tag{E6}$$

From equation (14g), neglecting the radial variation in entropy,

$$V_{z,t}\frac{dV_{z,t}}{dr_t}=-\frac{1}{r_t^2}\zeta_t\frac{d\zeta_t}{dr_t}$$

For station 1, from equation (E5)

$$V_{z,1}\frac{dV_{z,1}}{dr_1}=-\frac{1}{r_1^2}\left(\frac{\omega r_1^2}{2}-\frac{r_{1,t}\delta_t U_{1,t}}{2}\right)\omega r_1=-U_{1,t}^2\left(\frac{1}{2}\frac{r_1}{r_{1,t}^2}-\frac{\delta_t}{2r_1}\right)$$

Integrating from r_h to r_1 yields

$$\left(\frac{V_{z,1}}{U_{1,t}}\right)^2=\left(\frac{V_{z,1,h}}{U_{1,t}}\right)^2+\delta_t\log_e\frac{r_1}{r_{1,h}}-\frac{1}{2}\left(\frac{r_1^2}{r_{1,t}^2}-\frac{r_{1,h}^2}{r_{1,t}^2}\right) \tag{E7}$$

which is the same as equation (D13). For station 2,

$$V_{z,2}\frac{dV_{z,2}}{dr_2}=-\frac{1}{r_2^2}\left(\frac{\omega r_1^2}{2}+\frac{r_{1,t}\delta_t U_{1,t}}{2}\right)\omega r_1\frac{dr_1}{dr_2}$$

$$V_{z,2}\,dV_{z,2}=-\frac{r_1}{2r_2^2}(\omega^2r_1^2+\delta_t U_{1,t}^2)dr_1$$

$$=-\frac{r_1^2}{2r_2^2}U_{1,t}^2\left(\frac{r_1}{r_{1,t}}+\frac{\delta_t}{\frac{r_1}{r_{1,t}}}\right)d\left(\frac{r_1}{r_{1,t}}\right)$$

Integrating from $r_{1,h}$ to r_1 yields

$$\left(\frac{V_{z,2}}{U_t}\right)^2=\left(\frac{V_{z,2,h}}{U_t}\right)^2-\int_{\frac{r_{1,h}}{r_{1,t}}}^{\frac{r_1}{r_{1,t}}}\left(\frac{r_1}{r_2}\right)^2\left(\frac{r_1}{r_{1,t}}+\frac{\delta_t}{\frac{r_1}{r_{1,t}}}\right)d\left(\frac{r_1}{r_{1,t}}\right) \quad \text{(E8)}$$

which differs from equation (D13).

The density distribution at station 1 is the same as the simplified radial approximation, whereas that at station 2 is obtained by using equation (D14). The solution of this case is a process of successive approximations. Values of $r_2(r_1)$ obtained in the simplified radial approximation can be used here as the starting values. Then the distributions of $V_{\theta,2}$, $V_{z,2}$, ρ_2, and G_2 are calculated from the preceding equations, and new values of $r_2(r_1)$ are computed from equation (C5). Usually, only two or three cycles are necessary to obtain the correct value, because the difference between this case and the simplified-radial-equilibrium approximation of this type of design is small.

Infinite aspect ratio.—The first equation for the condition $G_1=G_2$ is the same as equation (E1). The second equation necessary to solve this case is a little more complicated than that in the previous type of design because $\frac{d\zeta}{dr}\neq 0$. If equation (34a) is used,

$$V_{z,1}\frac{dV_{z,1}}{dr}+V_{z,2}\frac{dV_{z,2}}{dr}=-\frac{1}{r^2}\left(\zeta_1\frac{d\zeta_1}{dr}+\zeta_2\frac{d\zeta_2}{dr}\right)$$

$$=-\frac{\omega}{r}(\zeta_1+\zeta_2)=-\omega^2 r$$

Then

$$V_{z,1}^2+V_{z,2}^2=-\omega^2r^2+\text{constant}$$

or

$$\frac{V_{z,1}^2}{U_t^2}+\frac{V_{z,2}^2}{U_t^2}=-\frac{r^2}{r_t^2}+\text{constant} \quad \text{(E10)}$$

In order to compare the result of this case with other cases, the same value of $V_{z,1,m}$ may be used. Then from equation (E1), $V_{z,2,m}$ is found, and the constant in equation (E10) is evaluated by using this set of $V_{z,1,m}$ and $V_{z,2,m}$. A few values of $V_{z,1}$ are assumed at any other given radius, with corresponding values of $V_{z,2}$ obtained from equation (E10). The correct values of $V_{z,1}$ and $V_{z,2}$ that will satisfy equation (E1) are obtained by interpolation.

After the distribution of axial velocity is known, the density distributions are obtained from equations (D11) and (D14), and pressure distributions, total enthalpy change, and air angles are obtained in the same manner as before.

APPENDIX F

APPROXIMATE VALUE OF RADIAL DISPLACEMENT ACROSS BLADE ROW HAVING FINITE ASPECT RATIO FOR GENERAL CASE IN WHICH ζ_1 AND ζ_2 ARE PRESCRIBED IN DESIGN AS FUNCTIONS OF r_1

In the latter part of appendix E, distribution of axial velocity is expressed in terms of known H, ζ, r_1, and $r_2(r_1)$. Alternatively, this distribution can be expressed in terms of radial displacement and its value determined by the simplified-radial-equilibrium calculation, for which $\Delta_e=0$. For a nontapered passage, it is seen from equation (14c) that

$$V_{z,1}\frac{dV_{z,1}}{dr_1}=V_{z,1,s}\frac{dV_{z,1,s}}{dr_1}+\frac{\Delta_e}{2}\left(\frac{\pi}{L}\right)^2V_{z,1}^2 \quad \text{(F1)}$$

and

$$V_{z,2}\frac{dV_{z,2}}{dr_1}=V_{z,2,s}\frac{dV_{z,2,s}}{dr_1}-\frac{\Delta_e}{2}\left(\frac{\pi}{L}\right)^2(V_{z,2})^2\frac{dr_2}{dr_1}+\zeta_2\frac{d\zeta_2}{dr_1}\left(\frac{1}{r_1^2}-\frac{1}{r_2^2}\right) \quad \text{(F2)}$$

By substituting $(r_1+\Delta_e)$ for r_2, expanding $\left(1+\frac{\Delta_e}{r_1}\right)^{-2}$ in a binomial series, and neglecting terms of greater order than $\left(\frac{\Delta_e}{r_1}\right)^2$, equation (F2) becomes

$$V_{z,2}\frac{dV_{z,2}}{dr_1}=V_{z,2,s}\frac{dV_{z,2,s}}{dr_1}-\frac{\Delta_e}{2}\left(\frac{\pi}{L}\right)^2(V_{z,2})^2\left(1+\frac{d\Delta_e}{dr_1}\right)+$$

$$\zeta_2\frac{d\zeta_2}{dr_1}\left(2\frac{\Delta_e}{r_1^3}\right)-\zeta_2\frac{d\zeta_2}{dr_1}\left(\frac{3\Delta_e^2}{r_1^4}\right) \quad \text{(F3)}$$

If $\Delta_e(r_1)$ is known, equations (F1) and (F3) may be solved as linear first-order differential equations in $V_{z,1}^2$ and $V_{z,2}^2$, respectively, giving (omitting the subscript 1 on r)

$$V_{z,1}^2=e^{\left(\frac{\pi}{L}\right)^2\int_{r_m}^{r}\Delta_e dr}\left[\int_{r_m}^{r}\left(\frac{d}{dr}V_{z1,s}^2\right)e^{-\left(\frac{\pi}{L}\right)^2\int_{r_m}^{r}\Delta_e dr}dr+V_{z,1,m}^2\right] \quad \text{(F4)}$$

and

$$V_{z,2}^2=e^{-\left(\frac{\pi}{L}\right)^2\varphi(r)}\left\{\int_{r_m}^{r}\left[\frac{d}{dr}V_{z,2,s}^2+\frac{2\Delta_e}{r^3}\frac{d}{dr}\zeta_2^2-\frac{3(\Delta_e)^2}{r^4}\frac{d}{dr}\zeta_2^2\right]e^{\left(\frac{\pi}{L}\right)^2\varphi(r)}dr+V_{z,2,m}^2\right\} \quad \text{(F5)}$$

where

$$\varphi(r)=\int_{r_m}^{r}\Delta_e\,dr+\frac{1}{2}\{(\Delta_e)^2-[\Delta_e(r_m)]^2\}$$

and subscript m may here refer to any radius between hub and tip.

For the limiting case of zero aspect ratio, the last term in equation (F1) approaches zero so that $V_{z,1}=V_{z,1,s}$, whereas $V_{z,2}$ is obtained by integrating equation (F3) with the third term neglected.

$$V_{z,2}^2=V_{z,2,s}^2-(V_{z,2,s,m}^2-V_{z,2,m}^2)+2\int_{r_m}^{r}\frac{\Delta_e}{r^3}\left(\frac{d}{dr}\zeta_2^2\right)dr-3\int_{r_m}^{r}\frac{(\Delta_e)^2}{r^4}\left(\frac{d}{dr}\zeta_2^2\right)dr \tag{F6}$$

When equation (F4) is integrated by parts and $\Delta_e(r_1)$ is replaced by $y_e\,g(r)$ as in equation (35), there is obtained

$$V_{z,1}^2=V_{z,1,s}^2+e^{\left(\frac{\pi}{L}\right)^2 y_e\varphi_1(r)}(V_{z,1,m}^2-V_{z,1,m,s}^2)-e^{\left(\frac{\pi}{L}\right)^2 y_e\varphi_1(r)}\int_{r_m}^{r}V_{z,1,s}^2\frac{d}{dr}e^{-\left(\frac{\pi}{L}\right)^2 y_e\varphi_1(r)}dr$$

in which

$$\varphi_1(r)=\int_{r_m}^{r}g(r)dr$$

If it is desired to compare the general case with other cases on the basis of the same $V_{z,1,m}$, then $V_{z,1,m}=V_{z,1,m,s}$. By the use of the mean-value theorem of integral calculus, the preceding equation can be written as

$$V_{z,1}^2-V_{z,1,s}^2=-e^{\left(\frac{\pi}{L}\right)^2 y_e\varphi_1(r)}\overline{V_{z,1,s}^2}\left[e^{-\left(\frac{\pi}{L}\right)^2 y_e\varphi_1(r)}-1\right]=\overline{V_{z,1,s}^2}\left[e^{\left(\frac{\pi}{L}\right)^2 y_e\varphi_1(r)}-1\right] \tag{F7}$$

where $\overline{V_{z,1,s}^2}$ is a mean value of $V_{z,1,s}^2$ between r and r_m, the mean depending on the choice of the function $g(r)$. If the approximation is made in letting $V_{z,2,m}=V_{z,2,m,s}$, equation (F5) may be written as

$$V_{z,2}^2-V_{z,2,s}^2=\overline{V_{z,2,s}^2}\left[e^{-\left(\frac{\pi}{L}\right)^2 y_e\varphi_2(r)}-1\right]+y_e\varphi_3(r)-y_e^2\varphi_4(r) \tag{F8}$$

where

$$\varphi_2(r)=\frac{\varphi(r)}{y_e}=\varphi_1(r)+\frac{1}{2}y_e\{[g(r)]^2-[g(r_m)]^2\}$$

$$\varphi_3(r)=e^{-\left(\frac{\pi}{L}\right)^2\varphi(r)}\int_{r_m}^{r}e^{\left(\frac{\pi}{L}\right)^2\varphi(r)}\frac{2g(r)}{r^3}\frac{d}{dr}\zeta_2^2\,dr$$

and

$$\varphi_4(r)=e^{-\left(\frac{\pi}{L}\right)^2\varphi(r)}\int_{r_m}^{r}e^{\left(\frac{\pi}{L}\right)^2\varphi(r)}\frac{3[g(r)]^2}{r^4}\frac{d}{dr}\zeta_2^2\,dr$$

The change in the distributions of $V_{z,1}$ and $V_{z,2}$ with the maximum displacement y_e for a given $g(r)$ is now determined by differentiating equations (F7) and (F8), assuming that r_m, $\overline{V_{z,1,s}^2}$, and $\overline{V_{z,2,s}^2}$ are independent of y_e

$$2\frac{d}{dy_e}\log_e V_{z,1}=\frac{\overline{V_{z,1,s}^2}}{V_{z,1}^2}\left(\frac{\pi}{L}\right)^2\varphi_1(r)e^{\left(\frac{\pi}{L}\right)^2 y_e\varphi_1(r)} \tag{F9}$$

$$2\frac{d}{dy_e}\log_e V_{z,2}=-\frac{\overline{V_{z,2,s}^2}}{V_{z,2}^2}\left(\frac{\pi}{L}\right)^2 e^{-\left(\frac{\pi}{L}\right)^2 y_e\varphi_2(r)}\left(\varphi_1(r)+y_e\{[g(r)]^2-[g(r_m)]^2\}\right)+\frac{\varphi_3(r)}{V_{z,2}^2}+\frac{y_e}{V_{z,2}^2}\frac{d\varphi_3(r)}{dy_e}-2y_e\frac{\varphi_4(r)}{V_{z,2}^2}-\frac{y_e^2}{V_{z,2}^2}\frac{d\varphi_4(r)}{dy_e} \tag{F10}$$

By subtracting equation (F10) from (F9) and neglecting three small terms containing y_e/V_z^2

$$\frac{d}{dy_e}\log_e\frac{V_{z,1}}{V_{z,2}}=\frac{1}{2}\left(\frac{\pi}{L}\right)^2\varphi_1(r)\left(\frac{\overline{V_{z,1,s}^2}}{V_{z,1}^2}e^{\left(\frac{\pi}{L}\right)^2 y_e\varphi_1(r)}+\frac{\overline{V_{z,2,s}^2}}{V_{z,2}^2}e^{-\left(\frac{\pi}{L}\right)^2 y_e\varphi_2(r)}\left\{1+y_e\frac{[g(r)]^2-[g(r_m)]^2}{\varphi_1(r)}\right\}\right)-\frac{1}{2}\frac{\varphi_3(r)}{V_{z,2}^2} \tag{F11}$$

The equation of continuity, equation (22), may be written as

$$\frac{\rho_1 V_{z,1}}{\rho_2 V_{z,2}}=\left[1+\frac{y_c g(r)}{r}\right]\left[1+y_c\frac{d}{dr}g(r)\right] \tag{F12}$$

by replacing r_2 with $r_1+y_c\,g(r)$. It is here assumed that the displacement Δ_c for the continuity equation has the same form as, but may differ in magnitude from, Δ_e. If the variation of $\rho_1/\rho_2(r)$ with y_c is neglected, that is, the density distribution is assumed to be determined primarily by the tangential velocity distribution, differentiation with respect to y_c for a given $g(r)$ gives

$$\frac{d}{dy_c}\log_e\frac{V_{z,1}}{V_{z,2}}=\frac{\frac{g(r)}{r}}{1+y_c\frac{g(r)}{r}}+\frac{\frac{d}{dr}g(r)}{1+y_c\frac{d}{dr}g(r)} \tag{F13}$$

If the same distribution of $V_{z,1}$ and $V_{z,2}$ satisfies both the continuity and equilibrium equations, y_c is a function of y_e determined by the differential equation, which is obtained by dividing equation (F11) by equation (F13):

$$\frac{dy_c}{dy_e}=\frac{1}{2}\frac{\left(\frac{\pi}{L}\right)^2\varphi_1(r)}{\frac{\frac{g(r)}{r}}{1+y_c\frac{g(r)}{r}}+\frac{\frac{d}{dr}[g(r)]}{1+y_c\frac{d}{dr}[g(r)]}}\left(\frac{\overline{V_{z,1,s}^2}}{V_{z,1}^2}e^{\left(\frac{\pi}{L}\right)^2 y_e\varphi_1(r)}+\frac{\overline{V_{z,2,s}^2}}{V_{z,2}^2}e^{-\left(\frac{\pi}{L}\right)^2 y_e\varphi_2(r)}\left\{1+y_e\frac{[g(r)]^2-[g(r_m)]^2}{\varphi_1(r)}\right\}-\frac{\varphi_3(r)}{V_{z,2}^2\left(\frac{\pi}{L}\right)^2\varphi_1(r)}\right) \tag{F14}$$

In order to evaluate equation (F14), the form of $g(r)$, which is implicit in the equations used, must be found. An order-of-magnitude result may be obtained, however, by equating the right side of equation (F14) to a constant $-K^2$ and determining the value of the constant from the boundary conditions on $g(r)$. Because this assumption involves setting dy_c/dy_e equal to a constant, it is equivalent to the assumption already stated that for the selected $\Delta_e=y_e\,g(r)$, the corresponding Δ_c differs only in amplitude. In order to obtain the order-of-magnitude result, the right side of equation (F14) is simplified by

(a) Setting the first two terms in the bracket equal to 2

(b) Considering the terms involving y_c and y_e negligible when they are compared with unity

(c) Ignoring the last term in the bracket because it contains $V_{z,2}^2\left(\frac{\pi}{L}\right)^2$ in the denominator (If equation (F14) is written in terms of r/r_t instead of r, the term $\left(\frac{\pi}{L}\right)^2$ becomes $\left(\frac{\pi r_t}{L}\right)^2$, which is about 250 for $A=2$ and $\frac{r}{r_t}=0.6$.)

As a result of this simplification, equation (F14) becomes

$$\frac{dy_c}{dy_e}=\frac{\left(\frac{\pi}{L}\right)^2\varphi_1(r)}{\frac{g(r)}{r}+\frac{d}{dr}g(r)}=-K^2 \tag{F15}$$

Rewriting equation (F15) gives

$$-\left(\frac{\pi}{L}\right)^2\frac{1}{K^2}\varphi_1(r)=\frac{g(r)}{r}+\frac{d}{dr}g(r) \tag{F16}$$

When equation (F16) is differentiated with respect to r and the relation $\frac{d}{dr}\varphi_1(r)=g(r)$ is used,

$$\frac{d^2}{dr^2}g(r)+\frac{1}{r}\frac{d}{dr}g(r)+\left[\left(\frac{\pi}{LK}\right)^2-\frac{1}{r^2}\right]g(r)=0$$

This equation gives $g(r)$ as a Bessel function of the first order and argument (π/LK). The value of (π/LK), and thus of K, is determined by the boundary conditions $g(r_h)=g(r_t)=0$. In order that $g(r)$ have a single maximum, the first eigenvalue of this boundary-value problem must be taken. A satisfactory approximation to this solution may be obtained without involving Bessel functions by replacing $g(r)/r$ in equation (F16) by $g(r)/r_m$, differentiating, and solving:

$$g(r)=e^{-\frac{r}{2r_m}}(K_1\cos lr+K_2\sin lr)$$

where

$$l=\sqrt{\left(\frac{\pi}{L}\right)^2\frac{1}{K^2}-\frac{1}{(2r_m)^2}}$$

The boundary conditions are determined by using the first eigenvalue for K,

$$K=\frac{\pi}{r_t-r_h}$$

$$g(r)=K_3e^{-\frac{r}{2r_m}}\sin\frac{r-r_h}{r_t-r_h}\pi \tag{F17}$$

and therefore,

$$\left(\frac{\pi}{L}\right)^2\frac{1}{K^2}=\frac{\pi^2}{(r_t-r_h)^2}+\frac{1}{4r_m^2}\approx\frac{\pi^2}{(r_t-r_h)^2}$$

(This approximate equality is correct within 1 percent for $(r_h/r_t)>0.5$.) Substituting this result in equation (F15) gives

$$\frac{dy_c}{dy_e}=-K^2=-\left(\frac{r_t-r_h}{L}\right)^2=-A^2 \tag{F18}$$

In this very rough approximation, dy_c/dy_e is therefore equal to minus the square of the aspect ratio. By integrating equation (F18) and by letting $y_{c,s}$ equal the value of y_c corresponding to $y_e=0$ (simplified-radial-equilibrium approximation),

$$y_c=y_{c,s}-A^2y_e \tag{F19}$$

A solution corresponds to $y_c=y_e=y$, which when substituted into equation (F18) gives

$$y=\frac{y_{c,s}}{1+A^2}$$

or

$$\Delta=\frac{\Delta_{c,s}}{1+A^2} \tag{37}$$

APPENDIX G

EQUATIONS FOR FINITE-ASPECT-RATIO CALCULATION

In the numerical example of the symmetrical-velocity-diagram and constant-total-enthalpy compressor, computation is made for a blade-row aspect ratio of 2, with a prescribed simple sinusodial radial-flow path. Inasmuch as the term containing radial variation of entropy is not considered, substituting equation (E5) into (14c) gives

$$\frac{dV_{z,1}^2}{dr_1}+\left(\frac{\pi}{L}\right)^2 (r_1-r_2)V_{z,1}^2=-U_{1,t}^2\left(\frac{r_1}{r_{1,t}^2}-\frac{\delta_t}{r_1}\right) \tag{G1}$$

and

$$\frac{dV_{z,2}^2}{dr_2}-\left(\frac{\pi}{L}\right)^2 (r_1-r_2)V_{z,2}^2=-U_{1,t}^2\frac{r_1}{r_2^2}\left(\frac{r_1^2}{r_{1,t}^2}+\delta_t\right)\frac{dr_1}{dr_2} \tag{G2}$$

From the relation

$$\frac{r_1-r_2}{L^2}=\frac{1}{r_t}\left(\frac{A}{1-\frac{r_h}{r_t}}\right)^2\left(\frac{r_1}{r_t}-\frac{r_2}{r_t}\right)$$

and integrating equations (G1) and (G2) from r_h to r, there results

$$\left(\frac{V_{z,1}}{U_t}\right)^2=e^{-\left(\frac{\pi A}{1-\frac{r_h}{r_t}}\right)^2\int_{\frac{r_h}{r_t}}^{\frac{r_1}{r_t}}\left(\frac{r_1}{r_t}-\frac{r_2}{r_t}\right)d\left(\frac{r_1}{r_t}\right)}\left[\left(\frac{V_{z,1,h}}{U_t}\right)^2-\int_{\frac{r_h}{r_t}}^{\frac{r}{r_t}}e^{\left(\frac{\pi A}{1-\frac{r_h}{r_t}}\right)^2\int_{\frac{r_h}{r_t}}^{\frac{r_1}{r_t}}\left(\frac{r_1}{r_t}-\frac{r_2}{r_t}\right)d\left(\frac{r_1}{r_t}\right)}\left(\frac{r_1}{r_t}-\delta_t\frac{r_t}{r_1}\right)d\left(\frac{r_1}{r_t}\right)\right] \tag{G3}$$

and

$$\left(\frac{V_{z,2}}{U_t}\right)^2=e^{\left(\frac{\pi A}{1-\frac{r_h}{r_t}}\right)^2\int_{\frac{r_h}{r_t}}^{\frac{r_2}{r_t}}\left(\frac{r_1}{r_t}-\frac{r_2}{r_t}\right)d\left(\frac{r_2}{r_t}\right)}\left[\left(V_{\frac{z,2,h}{U_t}}\right)^2-\int_{\frac{r_h}{r_t}}^{\frac{r_1}{r_t}}e^{-\left(\frac{\pi A}{1-\frac{r_h}{r_t}}\right)^2\int_{\frac{r_h}{r_t}}^{\frac{r_2}{r_t}}\left(\frac{r_1}{r_t}-\frac{r_2}{r_t}\right)d\left(\frac{r_2}{r_t}\right)}\left(\frac{r_1}{r_2}\right)^2\left(\frac{r_1}{r_t}+\delta_t\frac{r_t}{r_1}\right)d\left(\frac{r_1}{r_t}\right)\right] \tag{G4}$$

With this set of equations replacing (E7) and (E8), the rest of the calculation is the same as in the zero-aspect-ratio case. Equation (37) is used as starting value and by appropriate interpolation after two cycles of calculation the third or fourth cycle usually gives sufficient accuracy.

REFERENCES

1. Ruden, P.: Investigation of Single Stage Axial Fans. NACA TM 1062, 1944.
2. Eckert, and Korbacher: The Flow through Axial Turbine Stages of Large Radial Blade Length. NACA TM 1118, 1947.
3. Kahane, A.: Investigation of Axial-Flow Fan and Compressor Rotors Designed for Three-Dimensional Flow. NACA TN 1652, 1948.
4. Lamb, Horace: Hydrodynamics. Cambridge Univ. Press, 6th ed., 1932, articles 10, 329, 358.
5. Cope, W. F.: The Equations of Hydrodynamics in Their Very General Form. R. & M. No. 1903, British A.R.C., Nov. 1942.
6. Vazsonyi, Andrew: On Rotational Gas Flows. Quarterly Appl. Math., vol. 3, no. 1, April 1945, pp. 29–37.
7. Lorenz, H.: Theorie und Berechnung der Vollturbinen und Kreiselpumpen. V.D.I. Zeitschr., Bd. 49, Nr. 41, Okt. 14, 1905, S. 1670–1675.
8. Stodola, A.: Steam and Gas Turbines. Vol. II. McGraw-Hill Book Co., Inc., 1927. (Reprinted, Peter Smith (New York), 1945, pp. 990–991.)
9. Bauersfeld, W.: Zuschrift an die Redaktion. V.D.I. Zeitschr., Bd. 49, Nr. 49, Dez. 9, 1905, S. 2007–2008. (Written discussion of reference 7.)
10. Sinnette, John T., Jr., Schey, Oscar W., and King, J. Austin: Performance of NACA Eight-Stage Axial-Flow Compressor Designed on the Basis of Airfoil Theory. NACA Rep. 758, 1943.
11. Pochobradsky, B.: Effect of Centrifugal Force in Axial-Flow Turbines. Engineering, vol. 163, no. 4234, March 21, 1947, pp. 205–207.
12. Howell, A. R.: Fluid Dynamics of Axial Compressors. War Emergency Issue No. 12 pub. by Inst. Mech. Eng. (London), 1945. (Reprinted in U. S. by A.S.M.E., Jan. 1947, pp. 441–452.)

U. S. GOVERNMENT PRINTING OFFICE: 1950

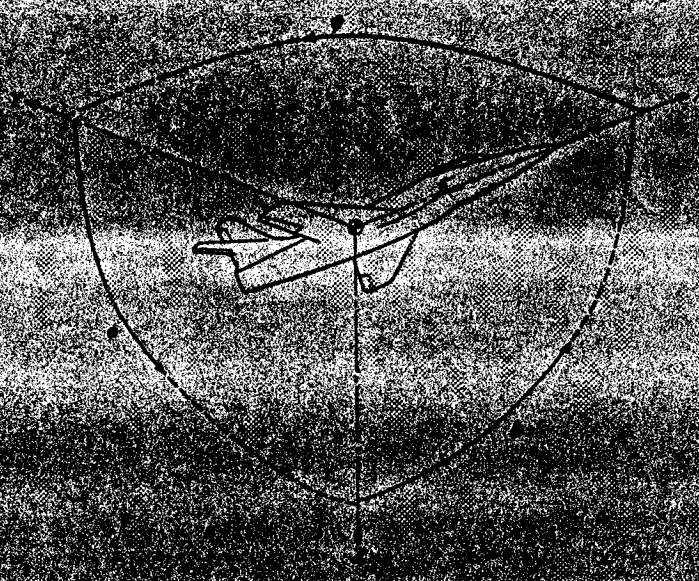

Positive directions of axes and angles (forces and moments are shown by arrows)

Axis		Force (parallel to axis) (symbol)	Moment about axis		Angle		Velocities	
Designation	Symbol		Designation	Symbol	Positive direction	Designation	Symbol	Linear (component along axis)	Angular
Longitudinal	X	X	Rolling	L	$Y \longrightarrow Z$	Roll	ϕ	u	p
Lateral	Y	Y	Pitching	M	$Z \longrightarrow X$	Pitch	θ	v	q
Normal	Z	Z	Yawing	N	$X \longrightarrow Y$	Yaw	ψ	w	r

Absolute coefficients of moment

$C_l = \frac{L}{qbS}$ (rolling) $\quad C_m = \frac{M}{qcS}$ (pitching) $\quad C_n = \frac{N}{qbS}$ (yawing)

Angle of set of control surface (relative to neutral position), δ. (Indicate surface by proper subscript.)

4. PROPELLER SYMBOLS

D Diameter

p Geometric pitch

p/D Pitch ratio

V' Inflow velocity

V_s Slipstream velocity

T Thrust, absolute coefficient $C_T = \frac{T}{\rho n^2 D^4}$

Q Torque, absolute coefficient $C_Q = \frac{Q}{\rho n^2 D^5}$

P Power, absolute coefficient $C_P = \frac{P}{\rho n^3 D^5}$

C_s Speed-power coefficient $= \sqrt[5]{\frac{\rho V^5}{P n^2}}$

η Efficiency

n Revolutions per second, rps

ϕ Effective helix angle $= \tan^{-1}\left(\frac{V}{2\pi r n}\right)$

5. NUMERICAL RELATIONS

1 hp = 76.04 kg-m/s = 550 ft-lb/sec

1 metric horsepower = 0.9863 hp

1 mph = 0.4470 mps

1 mps = 2.2369 mph

1 lb = 0.4536 kg

1 kg = 2.2046 lb

1 mi = 1,609.35 m = 5,280 ft

1 m = 3.2808 ft